1961

Distribution of loads in beam and slab bridge floors

Joseph Harold Senne
Iowa State University

DISTRIBUTION OF LOADS IN BEAM AND SLAB BRIDGE FLOORS

by

Joseph Harold Senne, Jr.

A Dissertation Submitted to the
Graduate Faculty in Partial Fulfillment of
The Requirements for the Degree of
DOCTOR OF PHILOSOPHY

Major Subject: Structural Engineering

Approved:

Signature was redacted for privacy.

In Charge of Major Work

Signature was redacted for privacy.

Head of Major Department

Signature was redacted for privacy.

Dean of Graduate College

Iowa State University
Of Science and Technology
Ames, Iowa

1961

TABLE OF CONTENTS

TABLE OF CONTENTS (Continued)

INTRODUCTION

Description of Beam and Slab Bridges

The present trend in highway bridge design is toward structures consisting of reinforced concrete floor slabs supported by longitudinal stringers of steel wide-flange sections or prestressed concrete. This change from the old truss bridge in the 20 to 100 foot span class has resulted in lower fabrication costs, faster erection, and a cleaner looking structure. The building of expressways with their many grade separation intersections and multi-leveled interchanges has also increased use of this type of structure. In addition, long span truss bridges use the beam and slab floor system between traverse floor beams in the bridge.

In practice the longitudinal beams may be simply supported at the ends or continuous over several spans. In addition, they can be bonded to the concrete slab using shear lugs giving rise to a composite section in which the concrete also acts as part of the beam in the positive moment region. Even if no shear lugs are present, some limited bonding action usually takes place between the beam and slab.

The transverse spacing of beams is usually the same throughout the bridge, the exact spacing and number depending on the design economics. At present a spacing of 9 to 10 feet

for steel beams and from 5 to 7 feet for prestressed concrete is being used unless head-room requirements dictate a greater number of shallow beams.

Most slab and beam bridge floors also contain diaphragms or transverse beams that connect the longitudinal beams together, usually at the ends and at intermediate positions along the span such as the third or quarter points. The effects of these diaphragms are generally not taken into account when designing the beams. They may, however, depending on their stiffness, appreciably affect the load distribution to these members.

The reinforced concrete slab thickness may vary from 6 to 10 inches, depending on the loading and the number of stringers involved. The main reinforcement is placed in the transverse direction and is designed to carry both positive and negative moment in the slab. A small amount of reinforcement is also placed longitudinally to distribute the load and to prevent cracking due to shrinkage and temperature effects.

Highway Bridge Loads

There are many loads that must be considered in designing a highway bridge, the principal ones being dead load, live load, impact, and wind (2, pp. 7-9).

The total dead load consists of the weights of all materials used in the bridge structure such as beams, slabs,

curbs, railings, and present or future wearing surfaces that must be applied. Most designers divide the total dead load equally among all stringers after preliminary sizes have been determined. The actual distribution is more complicated than this, depending somewhat on the same principle as the distribution of live load and on construction procedures such as shoring the beams until the slab has hardened, thus allowing the dead as well as live load to be carried by composite action.

The actual live load may be composed of a mixture of vehicles of various wheel spacings and weights, traveling at different speeds and intervals. The present practice in this country is to use the AASHO specifications, which designate that either a design truck (wheel) loading or a uniform lane load plus a transverse line load be used in each lane, depending on the one which gives the greater bending moment in the slab or beam (2, pp. 10-15). The AASHO design truck consists of two different axle arrangements, each with three different weights. One of these uses a wheel spacing of 6 feet, with 14 feet between front and rear axle. Eighty percent of the load is considered to act on the rear axle, the remaining 20 percent on the front axle. These trucks are designated H10-44, H15-44, and H20-44, meaning that the total weight of each is 10, 15, and 20 tons, respectively. The other design truck is the same as the first except that a trailer axle

equal in weight to the rear axle is added with a variable spacing from 14 to 30 feet from the rear axle. These trucks are designated H15-S12-44 and H20-S16-44, meaning that the total weight of the truck is 15 and 20 tons on the tractors and 12 and 16 tons on the trailer axles, respectively.

The impact load applied to a bridge is expressed as a percentage of the live load. This percentage, known as the impact factor, is specified by AASHO (2, p. 17) as a function of the loaded length of the span in question. The AASHO formula is based on fatigue and varies from 15 percent for long spans to a maximum of 30 percent for short lengths. Strictly speaking, the impact factor is dependent not only on the length of span but on many other factors such as the speed of vehicles, natural frequency of the bridge and roughness of the roadway. In other words, impact is also a dynamic effect, not only one of fatigue.

Present Design Procedure

Currently most states use the AASHO specifications for design of slab and beam floor systems (2, pp. 22-25). These specifications define an effective width of slab for various spans, a live load moment formula for the design of the slab, and expressions for determining the maximum distribution of wheel loads to the beams.

In these specifications the effective width of slab is

expressed as a function of the span for single or tandem axles. Actually it is also dependent on slab thickness, the slab to beam stiffness ratio, and longitudinal reinforcement. The slab moment is given, using moment coefficients to obtain both positive and negative moments. The load distribution to the beams is based on the spacing of stringers. For example, the 1957 AASHO specifications state that the fraction of a wheel load to steel I-beams with a concrete slab for two or more traffic lanes shall be $\frac{S}{5.5}$ for interior and $\frac{S}{4.0 + 0.25S}$ for exterior stringers, where S = the spacing of stringers in feet.

Here again this distribution depends not only on spacing of the stringers but on slab and beam stiffness and the relative stiffness between individual beams. In addition, other effects such as torsion in the beams and longitudinal distribution of the load along the beams may have appreciable effects.

It is seen, therefore, that the AASHO specifications reduce to a very simplified state effects that are quite complex in nature. Also, since the specifications must cover a variety of bridges, they must understandably be quite conservative.

Present Investigation

Since the present AASHO specifications (1957) show considerable error in the load distribution to the beams of some

bridges, a number of methods have been developed by various individuals in order to obtain a closer correlation between design and test results. Some of these methods are discussed briefly in the Review of Literature section. In the present investigation another method is presented in which the distribution is solved in formula form for individual loadings instead of truck loadings. The solutions of the equations for the formulas are quite tedious but can be easily programmed and solved by a computer, thus eliminating the main disadvantage in solutions of this type. The theoretical results of this method were compared to tests using single loads on two laboratory test bridges and also with tests from two full-sized highway simple span bridges and two four span continuous highway bridges. The theory and test results are in close agreement; and as the use of electronic computers becomes more widespread in the highway field, this method will most likely take on more significance for the practical designer.

In addition to the load distribution analysis, some work was also conducted in connection with deflections and shearing forces in the slab. The effective width of slab in connection with slab design was also studied.

REVIEW OF LITERATURE

The problem of determining the distribution of loads in beam and slab bridge floors is not new. Research on the subject probably began in the middle of the eighteenth century and continued until the beginning of the twentieth century. During this period the theory of elasticity was developed and applied to various types of slabs and support conditions. In the early 1920's the increase in the number of motor vehicles and improvements in reinforced concrete construction gave increased impetus to research in this field.

In 1921, Westergaard (35) summarized previous theory and developed additional methods which helped lay the groundwork for present day investigations. It was realized at this point that while the theory of elasticity had furnished the basic plate equations applicable to slabs, the methods could only be applied to a very few problems due to the complexity of solution. Methods were then sought that could contain simplifying assumptions which would not introduce serious errors into the results. Actual tests, in addition, were conducted and in some cases empirical expressions for load distribution were developed.

Some of the first such tests to be conducted were those by Agg and Nichols (1) of Iowa State College (now Iowa State University) in 1919, in which bridges with steel stringers

and timber floors were used. This project was continued by Fuller and Caughey (5, 6, 9), utilizing bridges with timber and concrete floors placed on steel stringers. Strains were measured in the stringers for both dynamic and static truck loading.

These tests probably gave the first reliable data as to the actual distribution of load and may have helped establish the first formal specification of this type.

Although these concrete slab bridges were not designed for composite action with the steel stringers, it was noted at the time that the steel and concrete did act as a single unit.

In addition to research on load distribution, work was also being done on effective slab widths. This included an analytical study by Westergaard (34) in 1930 in determining the effective width of slabs for moment. His work indicated that the effective width of the slab was essentially the same for various distances from its supporting beam.

Some experimental work of a similar nature on reaction distribution for slabs on simple supports was done by Spangler (31, 32). He used slabs of various thicknesses, widths, and spans; and found that the effective width for shear at the edges along the reactions was essentially the same for loads in all positions along a line perpendicular to the supports.

Perhaps the most extensive investigation in connection

with concrete slabs supported by flexible beams has been carried out by the research teams at the University of Illinois, under the direction of Newmark and Siess (25). In this work, theoretical analyses were made (15), together with tests on many model bridges. From these tests it was determined that the load from the slab is distributed to the entire length of the beam in varying amounts. This distribution is curved and is usually considered in sinusoidal form. Also, the moments, reactions, and deflections produced from a sinusoidal load component are of the same sinusoidal variation.

A numerical method was developed by Newmark (22) which consisted of dividing the design load into components varying sinusoidally along the longitudinal axis, or expressing it as a Fourier series. In this way each term of the Series can be handled separately and then combined to get the total effect. The method, while accurate, is quite involved and has not been used extensively.

In 1946 a method was presented by Guyon (11) for computing transverse distribution of loads in a slab and beam floor system. His theory neglected the torsional stiffness of the beams but this was later taken into account by Massonnet (18, 19).

In brief, this method consists of replacing the structure by an equivalent continuous structure that has the same average flexural and torsional stiffness as the actual bridge.

The loads are then placed on the slab and distributed longitudinally in sinusoidal form. These loads are expressed as a Fourier Series and substituted into the fourth order biharmonic or general plate equation. This method, using simplifying assumptions, is probably easier to handle than Newmark's method; but it has not been used extensively in this country.

In 1956 a doctoral thesis by R. M. Holcomb (12) presented the results of extensive tests made on two full-sized bridges and two small laboratory test bridges. This research, sponsored by the Iowa State Highway Commission as Research Project HR-12, was done at Iowa State University. In addition to the experimental work done, a method for the solution of bending moments in the beams of slab and beam bridges was developed. The procedure was essentially the method of consistent deformations in which deflections at various points between the slab and beams are equated. Here, as in Newmark's work, a sinusoidal distribution of loading on some of the beams was used. This procedure, while simpler than Newmark's method, is still somewhat involved. The results obtained were substantially in agreement with the experimental results, and are considerably more accurate than the standard AASHO distribution specifications for loads on stringers.

In 1960 D. A. Linger (17) conducted tests on four bridges in the Des Moines, Iowa area. All bridges were of the slab

and beam type. Two of them used prestressed concrete beams, one had aluminum and the other steel wide-flange stringers.

Although the tests on these bridges dealt more with dynamic rather than static loading, data was taken for both types of load distribution. The result of these tests showed that at midspan the dynamic and static distributions were very nearly the same. Some differences did occur in the steel stringer bridge, however, which seemed to have been due to torsional vibration of the slab.

Both the aluminum and steel stringer bridges were studied by the author and are described more fully in the section on Experimental Investigation.

THEORETICAL INVESTIGATION

Discussion

As has been shown in the Review of Literature section, many methods have been devised for obtaining the load distributed to bridge stringers. These methods vary from complex solutions by the theory of elasticity to the simple AASHO specifications. It was felt that perhaps a solution could be developed in formula form that, although it might be tedious to evaluate by hand, could easily be programmed for computer solution. Such a solution was made.

Solutions to many slab problems can be solved by introducing certain simplifying assumptions which do not appreciably affect the final result. The assumptions used in the method presented are as follows:

1. The standard assumptions with regard to flexure theory in beams are valid.

2. The slab is considered non-isotropic; stress is transferred more in one direction than in the other. In concrete slabs, most of the load is transferred in the direction of primary reinforcement.

3. All load in the slab is carried directly by the beams.

4. Poisson's Ratio is neglected.

5. Torsion is neglected in both beams and slab.

6. The flexural rigidity of the beams is based on the composite steel and concrete sections; and that of the slab is based on gross section, neglecting reinforcement.

7. Maxwell's Law of Reciprocal Displacements is valid.

8. Superposition for loads, moments, and deflections is valid.

The last two assumptions, when checked experimentally, were found to be within the margin of instrumentation error.

The procedure for deriving the equations assumes that the slab distributes the load transversely to the beams, which then take portions of the load depending on their relative stiffness and position with respect to position of load. The slab can therefore be considered a cross beam of finite width on elastic supports. The method chosen as the most convenient for obtaining the distribution in formula form was the principle of least work. This principle, for a loaded indeterminate structure in equilibrium, states that the values of the redundants must be such that the internal work (internal strain energy) in the structure is a minimum. Or, in other words, the partial derivative of the total strain energy with respect to a redundant is equal to zero:

$$\frac{\partial Wi}{\partial R} = 0. \qquad (1)$$

This relationship was discovered by Castigliano in 1878 and is generally known as Castigliano's Second Theorem.

The use of this theorem requires the evaluation of the internal work (Wi) done in the beam. For beams in flexure the work done in bending is equal to one-half the bending moment (M) times the change in slope (θ) of the beam, or

$$dWi = \frac{1}{2} M d\theta \quad . \tag{2}$$

Since

$$d\theta = \frac{Mdx}{Ei} \quad , \tag{3}$$

the total internal work in the beam can be written as

$$Wi = \int_a^b \frac{1}{2} \frac{M^2 dx}{Ei} \quad . \tag{4}$$

The expression M contains the moments of redundant members in addition to the known loads on the beam, and the strain energy can now be minimized by setting the partial derivative of the work with respect to each redundant equal to zero:

$$\frac{\partial Wi}{\partial R} = \int_a^b \frac{M \partial M}{EI \partial R} dx = 0 \quad . \tag{5}$$

While the theory is general and may be used for direct stress, shear deformations, and torsion; only its application to flexure will be considered in the following development.

Notation

In the derivation below and throughout the text, the following terminology is used:

R_A = reaction of slab on the beam A (see Fig. 1)

R_B = reaction of slab on the beam B

R_C = reaction of slab on the beam C

R_D = reaction of slab on the beam D

P = concentrated loading (assumed unity)

a = transverse distance of concentrated load from beam A

S = spacing of beams

l' = distance between centers of outside beams

L = length of longitudinal beams center to center of supports

b = distance of load P from left support of beams

c = L - b

Wi = work, or internal strain energy, stored in a member subjected to load

$E_AI_A = K_A$ = flexural rigidity of beam A

$E_BI_B = K_B$ = flexural rigidity of beam B

$E_CI_C = K_C$ = flexural rigidity of beam C

$E_DI_D = K_D$ = flexural rigidity of beam D

$E_sI_s = K_E$ = flexural rigidity of beam E (slab)

$H = \frac{EI(beam)}{L\,E_sI_s}$

$$r = \frac{EI(\text{beam})}{EI(\text{diaphragm})}$$

Derivation of Slab-Beam Equations

The problem solved here is for a bridge with a slab supported by four beams with a unit load P placed at any point on the slab, making it an indeterminate structure with two redundants. The loading condition and diagram are shown in Fig. 1. R_A and R_B are assumed to be the redundants and are assumed positive when acting upward on the slab, or downward on the beam. A negative value of R_A, therefore, indicates a downward force on the slab and an upward force on the beam. From equilibrium conditions, R_C and R_D can be obtained in terms of R_A and R_B (see Fig. 1):

$$R_C = -3R_A + 3P - \frac{Pa}{S} - 2R_B \ , \tag{6}$$

$$R_D = 2R_A - 2P + \frac{Pa}{S} + R_B \ . \tag{7}$$

Writing the bending moment equations for the cross beam E (slab),

$$M_x \text{ from } R_A \text{ to } P = R_A x_1 \ , \tag{8}$$

$$M_x \text{ from } P \text{ to } R_B = R_A x_1 - P(x_1 - a) \ , \tag{9}$$

$$M_x \text{ from } R_B \text{ to } R_C = R_A x_1 - P(x_1 - a) + R_B(x_1 - S) \ , \tag{10}$$

$$M_x \text{ from } R_D \text{ to } R_C = R_C x_2 - 2R_A x_2 - 2Px_2 + \frac{Pax_2}{S} + R_B x_2 \ . \tag{11}$$

x_1 is measured from R_A to R_C

x_2 is measured from R_D to R_C

x_3 is measured from left support of beams to beam E

x_4 is measured from right support of beams to beam E

These values are then substituted in Equation 5:

$$\frac{\partial Wi_E}{\partial R_A} = \int_0^{l'} \frac{M \partial M dx}{E_s I_s \partial R_A} , \tag{12}$$

$$\frac{\partial Wi_E}{\partial R_B} = \int_0^{l'} \frac{M \partial M dx}{E_s I_s \partial R_B} ; \tag{13}$$

or for Case I when a is equal to or greater than 0, but less than or equal to S,

$$E_s I_s \frac{\partial Wi_E}{\partial R_A} = \int_0^{2S} R_A x_1^2 dx + \int_a^{2S} -P(x_1 - a)x_1 dx + \int_S^{2S} R_B(x_1 - S)x_1 dx$$

$$+ \int_0^{S} (4R_A x_2^2 - 4Px_2^2 + \frac{2Pax_2^2}{S} + 2R_B x_2^2)dx , \tag{14}$$

$$E_s I_s \frac{\partial Wi_E}{\partial R_B} = \int_S^{2S} \left[R_A x_1 - P(x_1 - a) + R_B(x_1 - S)\right](x_1 - S)dx$$

$$+ \int_0^{S} (2R_A - 2P + \frac{Pa}{S} + R_B)x_2^2 dx . \tag{15}$$

When the preceding equations are integrated between the proper limits and simplified, we obtain

$$\frac{\partial Wi_E}{\partial R_A} = \frac{1}{6E_sI_s}\left[24R_AS^3 + 9R_BS^3 - P(3S^3 - 4aS^2 + a^3)\right], \tag{16}$$

$$\frac{\partial Wi_E}{\partial R_B} = \frac{1}{12E_sI_s}\left[18R_AS^3 + 8R_BS^3 - P(18S^3 - 10aS^2)\right]. \tag{17}$$

In like manner for Case II when a is equal to or greater than S, but less than or equal to 2S,

$$\frac{\partial Wi_E}{\partial R_A} = \frac{1}{6E_sI_s}\left[24R_AS^3 + 9R_BS^3 - P(3S^3 - 4aS^2 + a^3)\right], \tag{18}$$

$$\frac{\partial Wi_E}{\partial R_B} = \frac{1}{12E_sI_s}\left[18R_AS^3 + 8R_BS^3 - P(16S^3 - 4aS^2 - 6a^2S + 2a^3)\right]. \tag{19}$$

Similarly, the expressions for energy stored in the beams can be obtained in terms of R_A and R_B.

For beam A:

$$E_AI_A\frac{\partial Wi_A}{\partial R_A} = \int_0^b \frac{R_Ac}{L}x_3\frac{\partial M}{\partial R_A}dx + \int_0^c \frac{R_Ac}{L}x_4\frac{\partial M}{\partial R_A}dx = \frac{c^2b^2R_A}{3L}. \tag{20}$$

Since R_B does not enter into the moment equation of beam A,

$$E_AI_A\frac{\partial Wi_A}{\partial R_B} = 0. \tag{21}$$

For beam B:

$$E_B I_B \frac{\partial Wi_B}{\partial R_A} = 0 \ , \tag{22}$$

$$E_B I_B \frac{\partial Wi_B}{\partial R_B} = \int_0^b \frac{R_B c}{L} x_3 \frac{\partial M}{\partial R_B} dx + \int_0^c \frac{R_B c}{L} x_4 \frac{\partial M}{\partial R_B} dx = \frac{c^2 b^2 R_B}{3L} \ . \tag{23}$$

For beam C:

$$E_C I_C \frac{\partial Wi_C}{\partial R_A} = \int_0^b \frac{R_C c}{L} x_3 \frac{\partial M}{\partial R_A} dx + \int_0^c \frac{R_C b}{L} x_4 \frac{\partial M}{\partial R_A} dx \ ,$$

$$= \frac{c^2 b^2}{L} (3R_A + 2R_B - 3P + \frac{Pa}{S} \ , \tag{24}$$

$$E_C I_C \frac{\partial Wi_C}{\partial R_B} = \int_0^b \frac{R_C c}{L} x_3 \frac{\partial M}{\partial R_B} dx + \int_0^c \frac{R_C b}{L} x_4 \frac{\partial M}{\partial R_B} dx \ ,$$

$$= \frac{2c^2 b^2}{3L} (3R_A + 2R_B - 3P + \frac{Pa}{S}) \ . \tag{25}$$

For beam D:

$$E_D I_D \frac{\partial Wi_D}{\partial R_A} = \int_0^b \frac{R_D c}{L} x_3 \frac{\partial M}{\partial R_A} dx + \int_0^c \frac{R_D b}{L} x_4 \frac{\partial M}{\partial R_A} dx \ ,$$

$$= \frac{2c^2 b^2}{3L} (2R_A + R_B - 2P + \frac{Pa}{S}), \tag{26}$$

$$E_D I_D \frac{\partial Wi_D}{\partial R_B} = \int_0^b \frac{R_D c}{L} x_3 \frac{\partial M}{\partial R_B} dx + \int_0^c \frac{R_D b}{L} x_4 \frac{\partial M}{\partial R_B} dx \ ,$$

$$= \frac{c^2 b^2}{3L} (2R_A + R_B - 2P + \frac{Pa}{S}). \tag{27}$$

The partial derivatives of the work in the individual members with respect to R_A and R_B can now be combined and set equal to zero.

$$\frac{\partial Wi}{\partial R_A} = Wi' \text{ beam E} + Wi' \text{ beam A} + Wi' \text{ beam B} + Wi' \text{ beam C} + Wi' \text{ beam D} = 0 . \quad (28)$$

$$\frac{\partial Wi}{\partial R_B} = Wi' \text{ beam E} + Wi' \text{ beam A} + Wi' \text{ beam B} + Wi' \text{ beam C} + Wi' \text{ beam D} = 0 . \quad (29)$$

In this case, Wi' represents the partial derivative of Wi with respect to the redundant in question. The final equations, derived after differentiating, integrating, and collecting terms, are shown in Fig. 1. Again, there are still two cases: one when a is equal to or greater than 0 but less than or equal to S, and the other when a is equal to or greater than S but less than or equal to 2S.

The final equations are in a form that is easy to program for the IBM 650 Computer. Solution by hand calculator of these equations required about one-half hour per point, as compared with four seconds for the electronic computer. After programming, over 1800 separate solutions were obtained for four different effective slab widths on the six different bridges investigated. Some of the values for the laboratory bridges are tabulated in the Appendix.

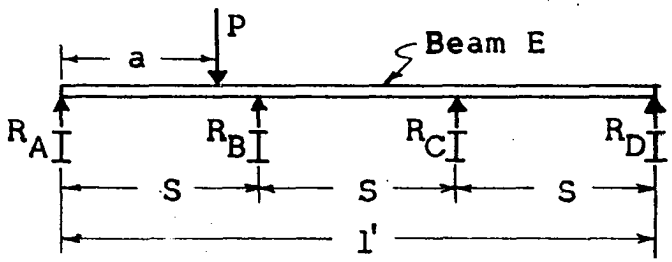

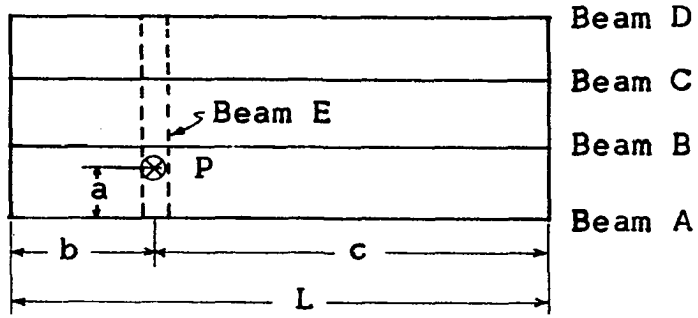

$$\frac{\partial W_i}{\partial R_A} = \left[\frac{4S^3}{K_E} + \frac{c^2b^2}{L}\left(\frac{1}{3K_A} + \frac{3}{K_C} + \frac{4}{3K_D}\right)\right] R_A + \left[\frac{3S^3}{2K_E} + \frac{c^2b^2}{L}\left(\frac{2}{K_C} + \frac{2}{3K_D}\right)\right] R_B +$$

$$P\left[\frac{(-24S^3 + 16aS^2 - a^3)}{6K_E} + \frac{c^2b^2}{L}\left(\frac{\frac{a}{S} - 3}{K_C} + \frac{2\left(\frac{a}{S} - 2\right)}{3K_D}\right)\right] = 0$$

$$\frac{\partial W_i}{\partial R_B} = \left[\frac{3S^3}{2K_E} + \frac{c^2b^2}{L}\left(\frac{2}{K_C} + \frac{2}{3K_D}\right)\right] R_A + \left[\frac{2S^3}{3K_E} + \frac{c^2b^2}{L}\left(\frac{1}{3K_B} + \frac{4}{3K_C} + \frac{1}{3K_D}\right)\right] R_B +$$

Case I only

$$P\left[\frac{5aS^2 - 9S^3}{6K_E} + \frac{c^2b^2}{L}\left(\frac{2\left(\frac{a}{S} - 3\right)}{3K_C} + \frac{\frac{a}{S} - 2}{3K_D}\right)\right] = 0$$

Case II only

$$\frac{(-8S^3 + 2aS^2 + 3a^2S - a^3)}{6K_E}$$

$$R_C = -3R_A + 3P - \frac{Pa}{S} - 2R_B$$

$$R_D = 2R_A - 2P + \frac{Pa}{S} + R_B$$

Use Case I when $0 < a \leq S$

Use Case II when $S \leq a < 2S$

Note: EI = K

Fig. 1. Final equations

EXPERIMENTAL INVESTIGATION

General Properties of Test Structures

As previously stated, the load distribution on six different bridges was studied. These consisted of two small laboratory bridges with simple spans of 10 and 25 feet, studied by the author theoretically and experimentally; two full-sized highway bridges with simple spans of 41.25 and 71.25 feet, included in the thesis of Holcomb (12), using another theoretical method of analysis; and one four span continuous aluminum beam highway bridge as well as a four span continuous steel beam bridge, both tested by Linger (17) with regard to dynamic action.

All tests were made using truck loadings except those by the author, which consisted of single concentrated loads. All bridges were analyzed by the author's proposed method and compared with the test results.

All six of these bridges were similar in some respects. Each had four longitudinal beams equally spaced and symmetrical in cross section. All inside curb faces were 6 inches outside the centerline of the exterior beams except those for the laboratory bridges, which were 2 inches, and that of the aluminum stringer bridge, which was 9 inches. All concrete slabs were approximately 8 inches thick except those for the

laboratory bridges, which were 2 inches. All bridges used shear lugs on the top flanges so that composite action would be developed between the beam and slab in the regions of positive moment. All bridges contained several relatively light intermediate diaphragms in each span. These diaphragms were not composite with the slab. The original calculations and design drawings for these bridges are on file with the Iowa State Highway Commission, Ames, Iowa. The 41.25 foot bridge is designated Design No. 3845, File 11744; the 71.25 foot is Design No. 3645, File 11744. The two continuous bridges carry traffic over the new interstate highway just northwest of Des Moines, Iowa. The aluminum stringer bridge is designated Design No. 3357A, Polk County; the steel stringer bridge is Design No. 3556, Polk County.

Laboratory Test Bridges

Description

These bridges both have a roadway width of 10 feet and span lengths of 10 and 25 feet each. The bridges are those used in the HR-12 Project and are located in the basement of the Engineering Experiment Station laboratory at Iowa State University.

Each bridge is approximately one-third the size of a standard highway bridge; however, changes in some of the dimensions for test purposes prevent them from being classified

as exact models of a prototype highway bridge. They do, however, represent a long span and short span bridge with somewhat thinner slabs and lighter beams than those used in actual design. The slabs of both bridges are about 2 1/4 inches thick and No. 5 smooth wires (.207 inch diameter) spaced on 2 inch centers are the primary reinforcement with two bent-up wires and a third wire top and bottom for both positive and negative moment. No. 5 wires spaced 7.7 inches on center or six wires per panel, all near the bottom, comprise the longitudinal reinforcement. Concrete coverage was 7/16 inch to the center of the main reinforcement, both top and bottom. This steel represents about half the amount that would be used if a one-third scale ratio had been maintained between model and prototype.

Each beam has constant cross section throughout, with the composite moment of inertia of the interior stringers approximately 1 1/2 times that of the exterior beams. Shear lugs welded to the tops of these beams insure composite action between steel and concrete. The reaction rods consist of 5/8 inch diameter vertical rods pinned at each end with horizontal pinned rods to prevent lateral movement. This arrangement gives the equivalent of a pinned condition at one end and a roller at the other.

General details of the 25 foot bridge are shown in Fig. 2 and properties of both bridges are listed in Table 1.

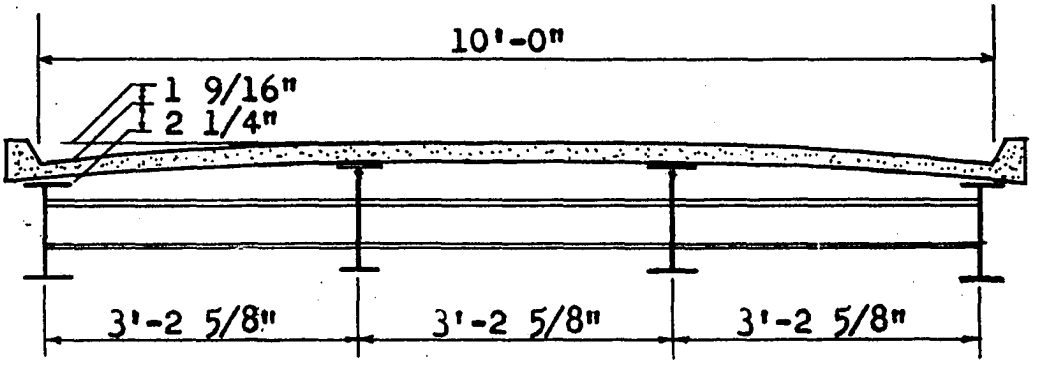

End elevation

Transverse reinforcement 0.207" diam. smooth rods, 2" o.c.
Two trussed bars and one smooth bar top and bottom.
Longitudinal reinforcement six bars per panel near bottom.

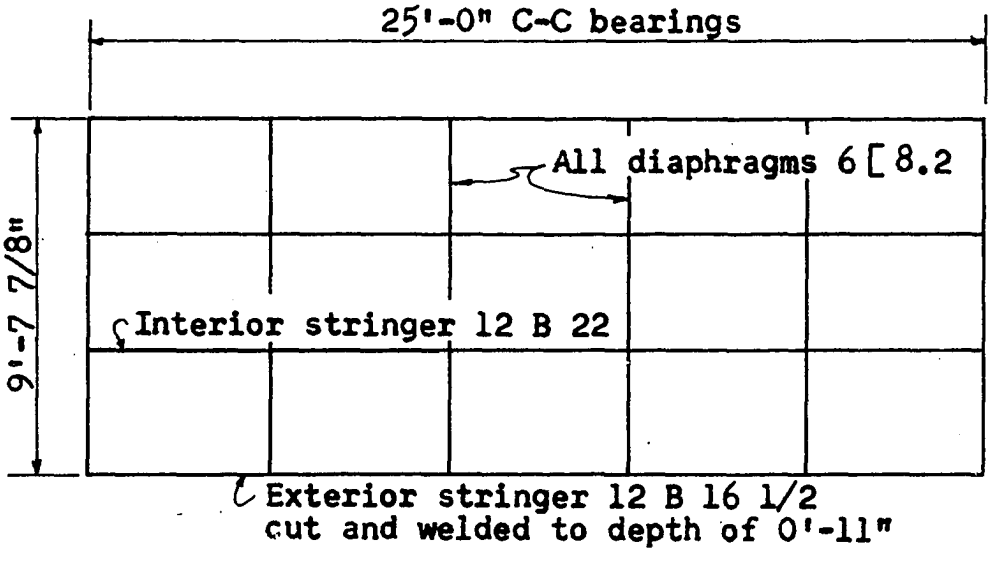

Fig. 2. Details of 25 foot bridge

In the HR-12 Project, concrete blocks were hung from the under side of the slab to make up the deficiency in dead load, to seat the reaction, and to prevent actual reversal of strains due to live load. This same arrangement was used in the present tests for similar reasons and to insure correlation between the readings obtained in the earlier HR-12 tests by Holcomb (12).

Complete detailed information on construction, determination of the modulus of elasticity of the steel beams, calibration of the reaction rods, and on the testing is in the files of the Iowa State Highway Commission.

Loading

The loadings used in the HR-12 Project were scaled-down truck loadings of 4,000 lbs for single axle loads, and 8,000 lbs for tandem axle loads. Dual wheels with tire sizes of 4.00-8, 2 feet between centers, were used. This represented almost an exact one-third scale ratio to the standard truck rear wheels (Fig. 4a).

In the present project, a single concentrated load used instead of wheel loads was applied by means of an hydraulic jack (Plate 1, 2). The loads applied were 5,000 and 10,000 lbs. A 15,000 lb load was sometimes applied near an interior beam when the load was at some distance from the midspan to get sizeable readings. The loads were placed on the 25 foot bridge according to a grid pattern of 1 foot longitudinally

Table 1. Properties of simple span laboratory bridges

Bridge, span, ft	10		25	
Span (L), in.	120		300	
Roadway width, ft	10		10	
Beam spacing (S), ft	3.22		3.22	
Slab thickness (t), in.	2.19		2.25	
Slab I_s $(t^3/12)$in.^{4}/in.	0.875		0.950	
Ratio $I_{int.}/I_{ext.}$ at midspan[a]	1.33		1.48	
Beam	B Int.	A Ext.	B Int.	A Ext.
I^b of beam, in.^{4} at midspan	67.2	50.6	379	256
EI of beam $(10)^9$ lbs/in.^{2} at midspan	1.98	1.49	11.14	7.52
EI of beam $(10)^9$ lbs/in.^{2} at end	--	--	--	--
I_{st}/c_{st} at midspan, in.^{3}	8.20	6.54	35.8	25.9
I_{st}/c_{st} at end, in.^{3}	--	--	--	--
$H = EI/LE_sI_s$ at midspan	5.1	3.9	10.7	7.2
r	0.057	0.075	0.034	0.051

[a]Composite interior and exterior beams

[b]Equivalent all-steel section, n = 8

and 9.67 inches transversely. The latter dimension corresponds to loading at the quarter points of the slab between beams (Fig. 3). The grid is numbered 0, 1, 2, 3, 4, etc. longitudinally; and A, B, C, D, etc. transversely. For example, a load placed at Grid F-10 would mean that the load is located 10 feet from the south end of the bridge, at the one-quarter point in the slab between the two interior beams, and east of the longitudinal centerline.

Instrumentation

In order to check the theoretical results, strains and deflections in the bridges were measured at a number of points. Strains in the steel and concrete were measured by electric strain gages. In the 25 foot bridge, 74 Type A-1 SR-4 gages were used on the steel beams, most of them on the bottom flanges, 18 inches on center, with a few near the neutral axis and on diaphragms. Eleven Type A-9 gages were used on the concrete slab above the stringers. In the center of the bridge, 45 A-1 gages were formed in a 3 x 3 foot grid pattern to measure strains in the concrete slab (see Plates 1, 2). In all, 130 gages were used to measure strains at 128 different grid locations of the load.

Sixteen dial gages, reading to 0.001 inches, were placed at the one-eighth points under the east interior and exterior stringers of the 25 foot bridge to measure deflections (Plate 4), while nine dial gages measured deflections on the

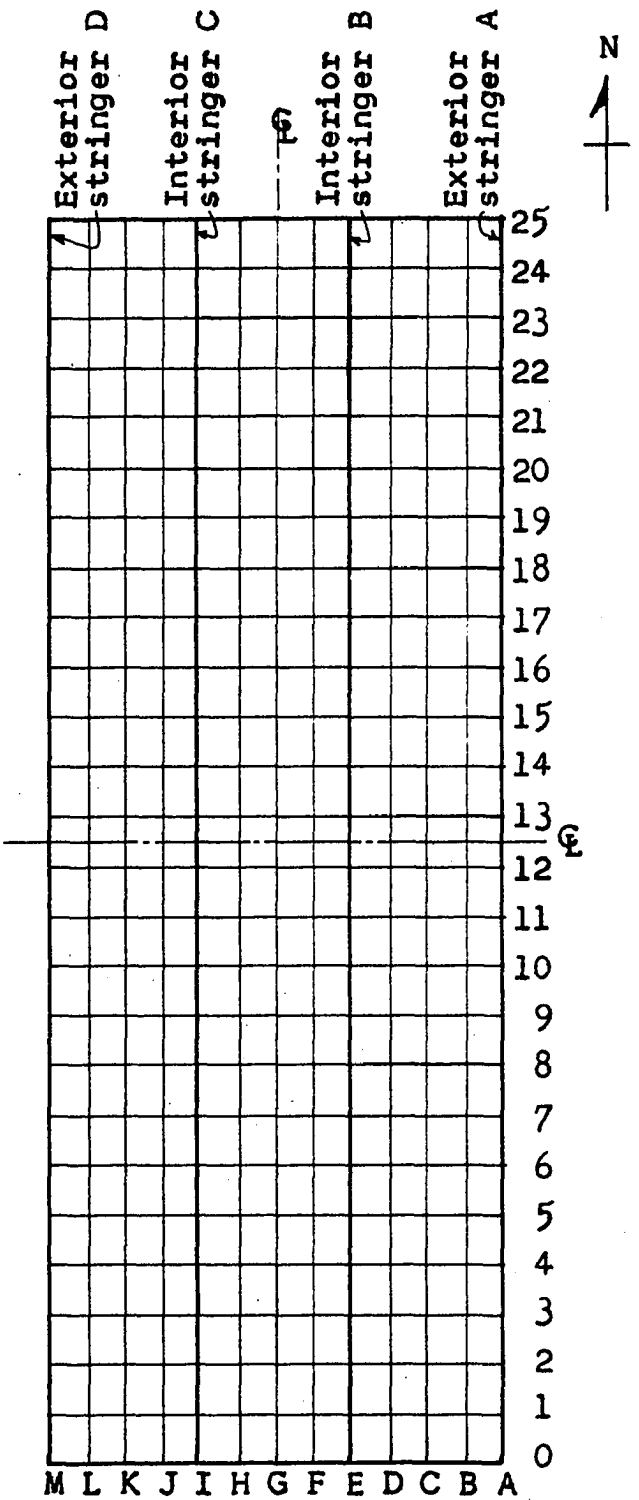

Fig. 3. Location of grid points on 25 foot bridge

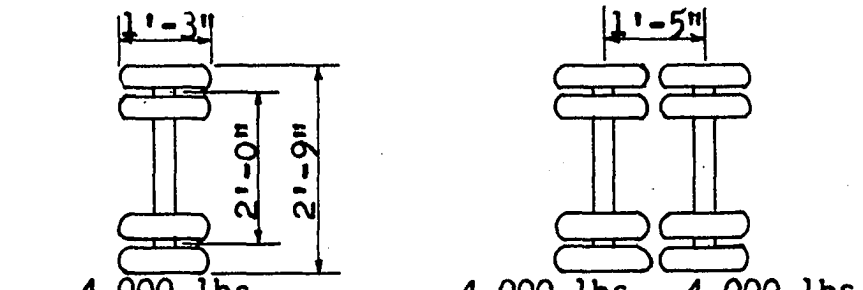

Fig. 4a. Trucks used on the 10 and 25 foot laboratory bridges in the HR-12 Project (Holcomb)

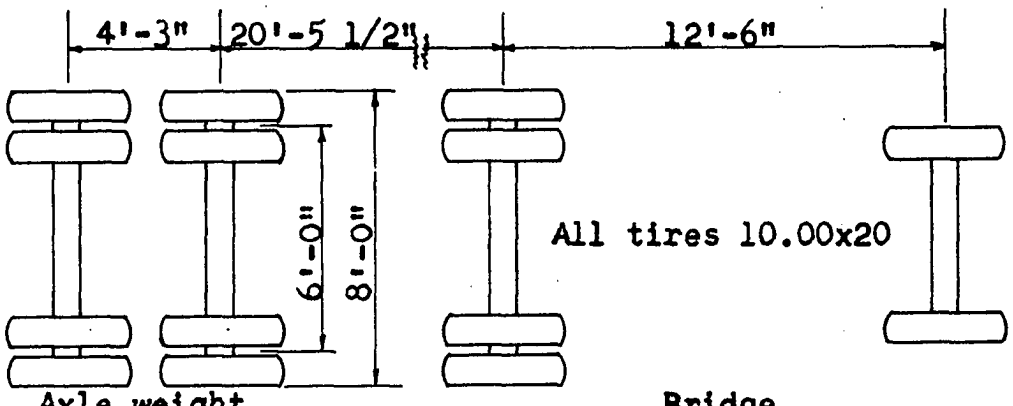

Axle weight				Bridge	
30,100	35,100 lbs	25,800 lbs	71.25 ft	7,000 lbs
32,000	34,300 lbs	24,300 lbs	41.25 ft	7,400 lbs

Fig. 4b. Truck loading used on the 41.25 and 71.25 foot simple span highway bridges in HR-12 Project (Holcomb)

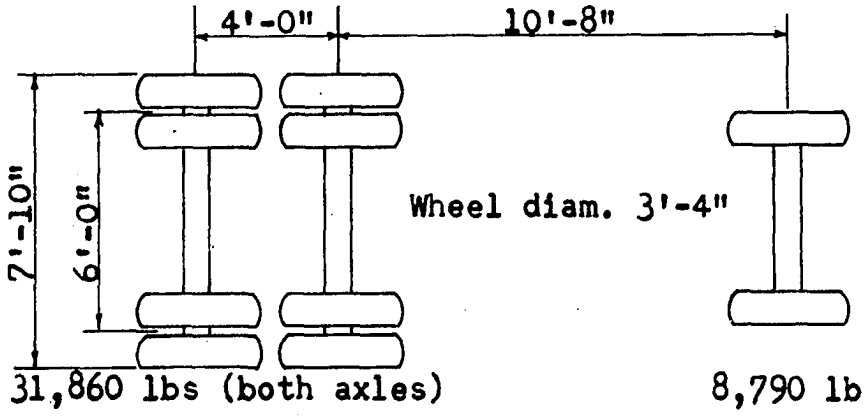

Fig. 4c. H-20 truck loading used on the 220 and 240 foot four span continuous bridges in Project 376-S (Linger)

Plate 1. 25 foot test bridge with loading arrangement

Plate 2. Dial and strain gage locations for central slab measurements

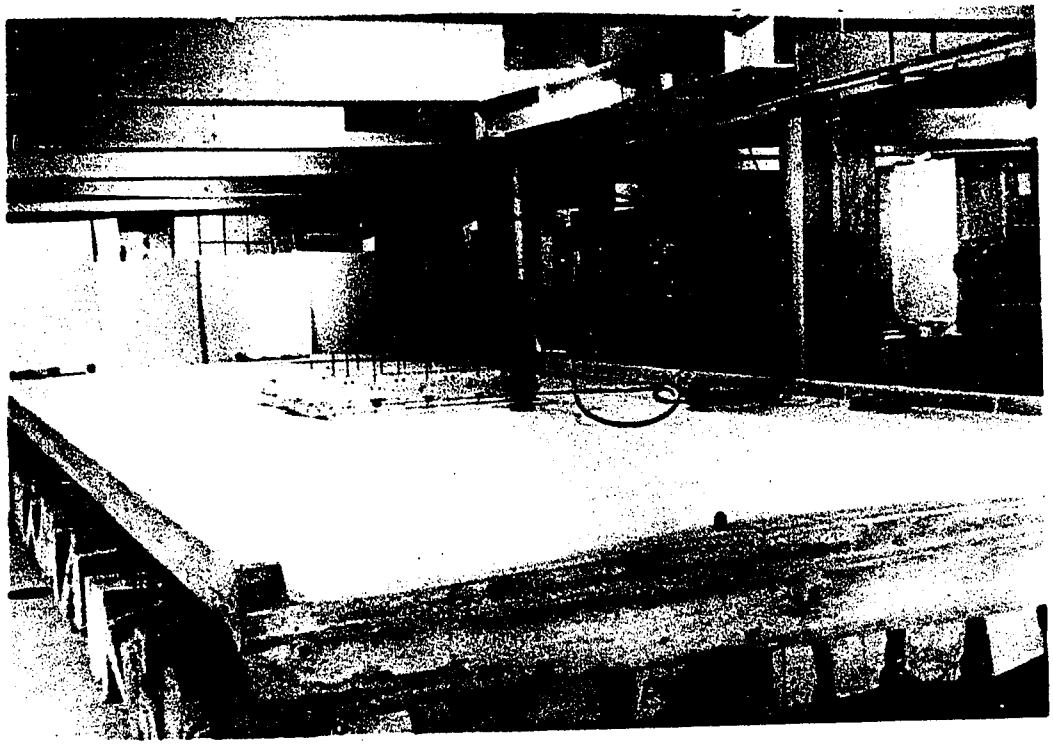

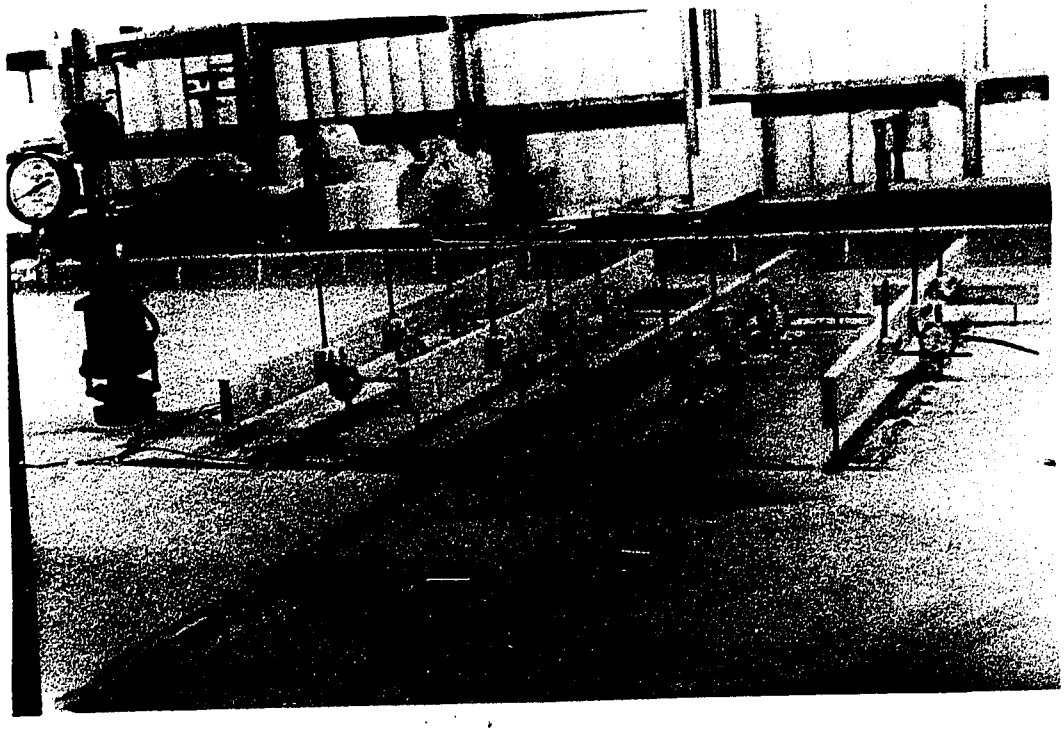

Plate 3. Switching unit and strain measuring equipment

Plate 4. Position of dial gages for measuring beam deflections

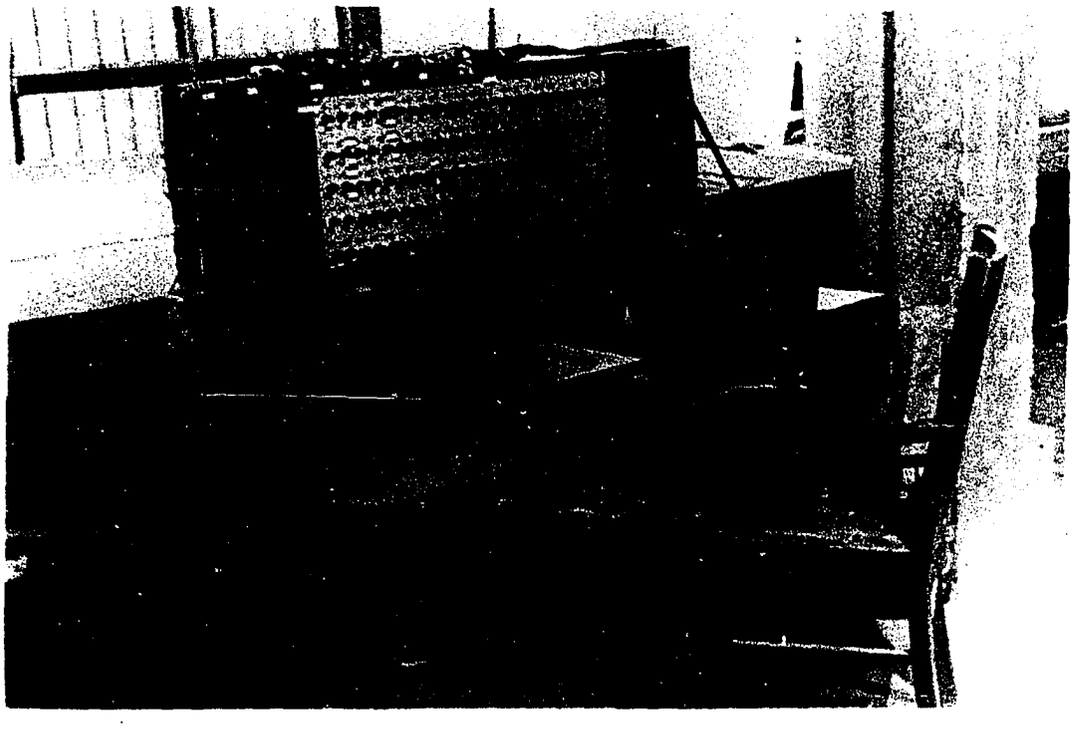

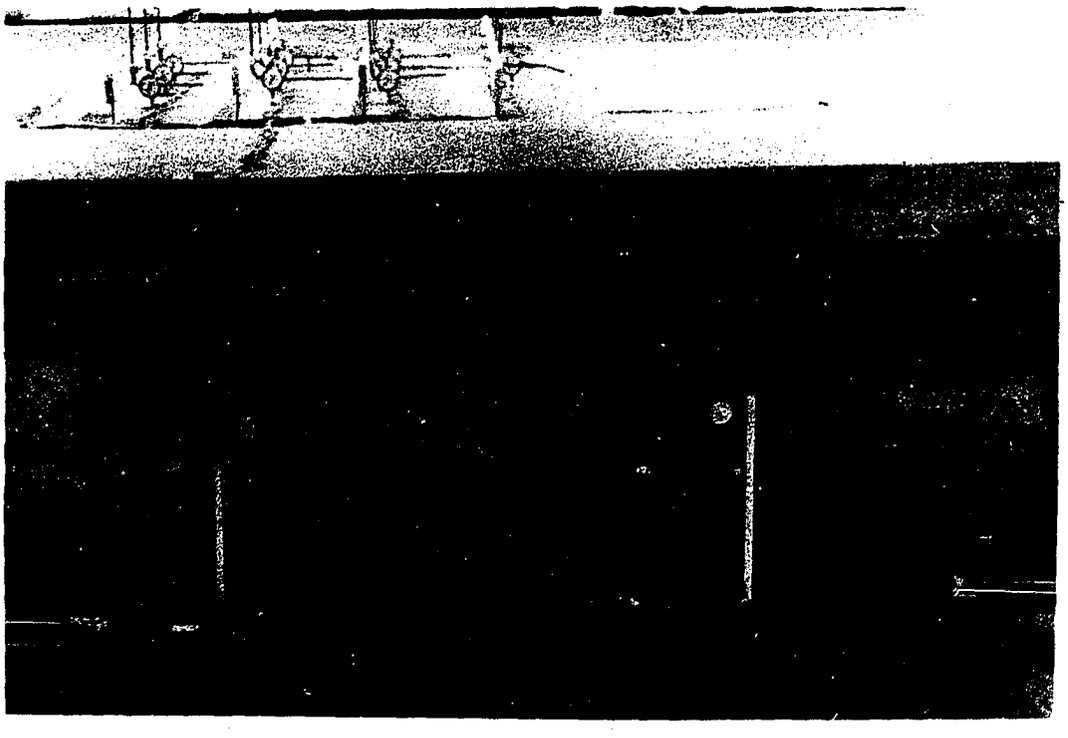

central grid pattern on the top of the slab (Plate 2).

Measurements were also taken for the determination of effective width for slab design. This was done by observing the relative deflection of the slab in the center of the 25 foot bridge as the load moved along the longitudinal centerline. The dial gages were supported so that the deflection of the slab due to beam deflection was canceled, as indicated in Fig. 6 and Plate 2, leaving only the relative slab deflection.

Most of the testing was done on the 25 foot bridge; the 10 foot bridge was tested at only a few critical points to provide a comparison of two different bridge lengths.

The strain gages on the steel were very stable. This was attributed to the fact that the bridges were located indoors, away from abrupt temperature changes and inclement weather that so plague the tests on outdoor structures. Difficulty was encountered with many of the strain gages on the concrete slab; some showed excessive readings while others were extremely small. This was no doubt due to the fact that the concrete surface had many hairline cracks, which is usual for such slabs. Efforts were made to place the gages so that they were not over a crack; but even then, gages near a crack would show small readings while a gage nearby, presumably over a crack, would show high values. The 6 inch A-9 gages generally worked satisfactorily, except that most of them showed slightly lower strains than were indicated by prediction.

Some shift was noted in the zero readings from day to day. Most of this probably was caused by humidity changes, which were due to a moist chamber located nearby.

Simple Span Highway Bridges (Field Spans)

Description

Each of these two bridges has a roadway width of 30 feet, the same curb dimensions, and the same crown. The spans are as previously stated: 41.25 feet and 71.25 feet. The end supports are curved bearing plates to allow rotation at the ends.

According to Holcomb (12, p. 90),

> The slabs vary slightly in thickness in the transverse sections. In the longitudinal sections the slab of the longer bridge is constant in thickness, but that of the shorter one is varied to compensate for dead load deflection, Fig. 14. An average thickness of 8.07 in. has been used throughout for the 71.25 ft. bridge. . . . The primary reinforcement of the slabs consists of 3/4 in. round straight bars at 8.5 in. center to center in both the top and bottom. According to the design drawings these bars were to have been placed at an average of 2 in. from the surfaces to the centers of the bars. Limited exploration disclosed, however, that they are actually severely displaced in the completed bridges. Longitudinal reinforcement consists of 13 3/4 in. round bars in each space between beams. Of these, 7 are near the top surface and 6 are near the bottom.

The properties of these bridges are listed in Table 2.

Loading

The test load for these bridges consisted of a single commercial semi-trailer truck loaded with pig iron to a total

Table 2. Properties of simple span highway bridges

Bridge, span, ft	41.25		71.25	
Span (L), in.	495		855	
Roadway width, ft	30		30	
Beam spacing (S), ft	9.69		9.69	
Slab thickness (t), in.	8.63		8.07	
Slab I_s $(t^3/12)$in.^{4}/in.	53.6		43.6	
Ratio $I_{int.}/I_{ext.}$ at midspan[a]	1.68		1.65	
Beam	B Int.	A Ext.	B Int.	A Ext.
I^b of beam, in.^{4} at midspan	16,600	9,900	45,500	27,500
I^b of beam, at end, in.^{4}	10,000	7,750	35,900	19,600
EI of beam $(10)^9$ lbs/in.^{2} at midspan	488	291	1,338	811
EI of beam $(10)^9$ lbs/in.^{2} at end	292	228	1,056	575
I_{st}/c_{st} at midspan, in.^{3}	620	395	1,450	928
I_{st}/c_{st} at end, in.^{3}	372	311	1,105	633
$H = EI/LE_sI_s$ at midspan	5.0	3.0	9.7	5.9
r	0.027	0.045	0.011	0.016

[a]Composite interior and exterior beams

[b]Equivalent all-steel section, n = 8

of 98,000 pounds. This load was distributed as follows: to the tandem tractor axles, which were 4.3 feet on center, approximately 65,500 pounds; to the rear truck axle, which was 20.45 feet ahead of the trailer axles, 25,300 pounds; to the front axle, which was 21.5 feet from the rear axle, 7,200 pounds (see Fig. 4b). This truck was positioned at several marked longitudinal and transverse locations on both bridges.

Instrumentation

Strains and deflections were taken by Holcomb at various points on the bridges for each position of the load. These strains were measured using SR-4 electric strain gages attached to the steel beams and diaphragms. Some of these were placed on the web of the beams in order to verify the location of the neutral axis. Deflections were measured along the stringers and transversely across the slab using dial gages.

Continuous Span Highway Bridges (Field Spans)

Description of aluminum stringer bridge

This structure is a 220 foot continuous four span bridge having an 8 inch concrete slab supported on four aluminum stringers. The outer spans are 41.25 feet and the inner 68.75 feet. The roadway is 30 feet wide with a 3 foot safety curb on both sides. The bridge was designed in 1957 using aluminum stringers to check the economy and design of a structure of this type. Additional properties are listed in Table 3.

Table 3. Properties of four span continuous aluminum stringer highway bridge

	Outer span		Inner span	
Bridge, span, ft	41.25		68.75	
Span (L), in.	495		495	
Roadway width, ft	30		30	
Beam spacing (S), ft	9.5		9.5	
Slab thickness (t), in.	8.00		8.00	
Slab I_s $(t^3/12)$in.^{4}/in.	42.6		42.6	
Ratio $I_{int.}/I_{ext.}$, midspan[a]	1.27		1.15	
Beam	B Int.	A Ext.	B Int.	A Ext.
I^b of beam, in.^{4} at midspan	28,547	22,355	44,155	38,449
I of beam, first int. support, in.^{4}	42,089	32,154	42,089	32,154
EI of beam, midspan, $(10)^9$ lbs/in.^{2}	294	230	454	396
EI of beam, at end, $(10)^9$ lbs/in.^{2}	434	331	434	331
I_{st}/c_{st}, midspan, in.^{3}	760	620	1,186	1,040
I_{st}/c_{st}, first int. support, in.^{3}	1,180	985	1,180	985
$H = EI/LE_sI_s$, midspan	3.72	2.92	3.42	3.01
r	0.097	0.169	0.062	0.098

[a]Composite interior and exterior beams

[b]Equivalent all-aluminum section, n = 2.75

Description of steel stringer continuous bridge

This 240 foot continuous four span structure has outer and inner spans of 52.5 and 67.5 feet, respectively. The slab is 7.5 inches thick and the roadway width is 28 feet plus a safety curb of 3 feet on both sides (Table 4).

Loading

The vehicles used by Linger (17) in these tests were designated Vehicle A and Vehicle B. Vehicle A is an International L-190 van-type truck used to check the Iowa State Highway Commission scales, and has a wheel base of 14 feet, 8 inches, with a gage of 6 feet. It weighs 40,650 pounds with 31,860 pounds on the rear tandem axle; in fact, it very nearly satisfies the AASHO specifications for the H-20-44 design truck (Fig. 4c). Vehicle B is a tandem axle truck with a 36 foot flat bed trailer. However, this truck was not used in determining load distribution, so is of little interest here.

Instrumentation

Since the tests performed on these field spans were primarily for the determination of dynamic effects, oscillograph recording equipment was used. This consisted of eight Brush universal amplifiers and direct writing recorders. SR-4 strain gages were cemented to the bottom flanges of the steel and aluminum stringers near points of maximum positive and

Table 4. Properties of four span continuous steel stringer highway bridge

	Outer span		Inner span	
Bridge, span, ft	52.5		67.5	
Span (L), in.	630		810	
Roadway width, ft	28		28	
Beam spacing (S), ft	9.0		9.0	
Slab thickness (t), in.	7.5		7.5	
Slab I_s $(t^3/12)$in.^{4}/in.	35.1		35.1	
Ratio $I_{int.}/I_{ext.}$, midspan[a]	0.92		0.92	
Beam	B Int.	A Ext.	B Int.	A Ext.
I[b] of beam, in.^{4} at midspan	16,071	17,353	15,976	17,353
I of beam, first int. support, in.^{4}	21,548	20,830	21,548	20,830
EI of beam, midspan, $(10)^9$ lbs/in.^{2}	482	520	479	515
EI of beam, at end, $(10)^9$ lbs/in.^{2}	649	626	649	626
I_{st}/c_{st}, midspan, in.^{3}	565	565	565	565
I_{st}/c_{st}, first int. support, in.^{3}	1,078	905	1,078	905
$H = EI/LE_sI_s$, midspan	7.22	7.85	5.62	6.11
r	0.028	0.026	0.028	0.026

[a]Composite interior and exterior beams

[b]Equivalent all-steel section, n = 10

negative moment. Additional gages were also placed on the concrete and on the webs in order to determine the exact position of the neutral axes.

The static tests were performed by having the loading vehicle creep across the bridge. This was done for several test lanes which ranged from contact with the curb to the middle of the bridge. For all these positions of the load, simultaneous strain readings were taken at the extreme bottom fibers of the beams. These values were then reduced by Linger to live load moments in each beam, and a percentage of each as compared to the total live load moment was obtained. This value was then taken as the live load distribution to each stringer. The method assumes that all moment diagrams are of the same shape. While this is not strictly true for single concentrated loads, it is more nearly correct when multiple wheel loads are used.

RESULTS AND DISCUSSION

General

The items investigated in this project can be listed briefly as follows:

1. Determination of effective slab width for design of the slab. This would correspond to the E value in the AASHO specifications (2, p. 24).
2. Determination of effective slab width for the distribution of loads from the slab to beams.
3. The shape of the moment diagram for the interior and exterior stringers, with a concentrated unit load at various positions on the slab.
4. Variation of shearing forces at the slab support.
5. Comparison of predicted and test results.
6. Method of handling superposition of loads.
7. Limitations of the equations.
8. Modification of the equations to include diaphragm and torsional stiffness.

Effective Slab Width

The effective width for slab design was studied by means of the slab deflection data taken at the center of the bridge. Using these deflections, influence curves were obtained, using

Maxwell's Law of Reciprocal Deflections, and are shown in Fig. 5. From these curves it can be seen that appreciable deflection extends about 4 feet on each side of the maximum point. However, the bulk is contained within the 30 inches specified by AASHO for a single axle load. The peak is quite high, due in all probability to the nature of the loading, which was transmitted to the slab through a lead plate 4 inches in diameter, a smaller area than that of a rubber-tired wheel. It should also be noted that the influence line for deflection at the quarter point of the slab at midspan, while much lower in value, has approximately the same effective width. The main reason for checking this width in addition to checking the AASHO specification was to compare it with the effective width for distribution to the beams.

In order to determine the effective slab width for the distribution of loads from the slab to beams, the equations in Fig. 1 were solved using effective slab widths ranging from 0.1L to L for the various bridges, L being the span length of the bridge. These values were then compared to the experimental results, and the most appropriate effective width chosen. For the two laboratory bridges, the 71.25 foot highway and the aluminum stringer bridge, an effective slab width of 0.8L was found to fit best the test results. Diagrams such as those shown in Figs. 7 and 8 were used in determining these widths. The best effective width for the 41.25 foot bridge and

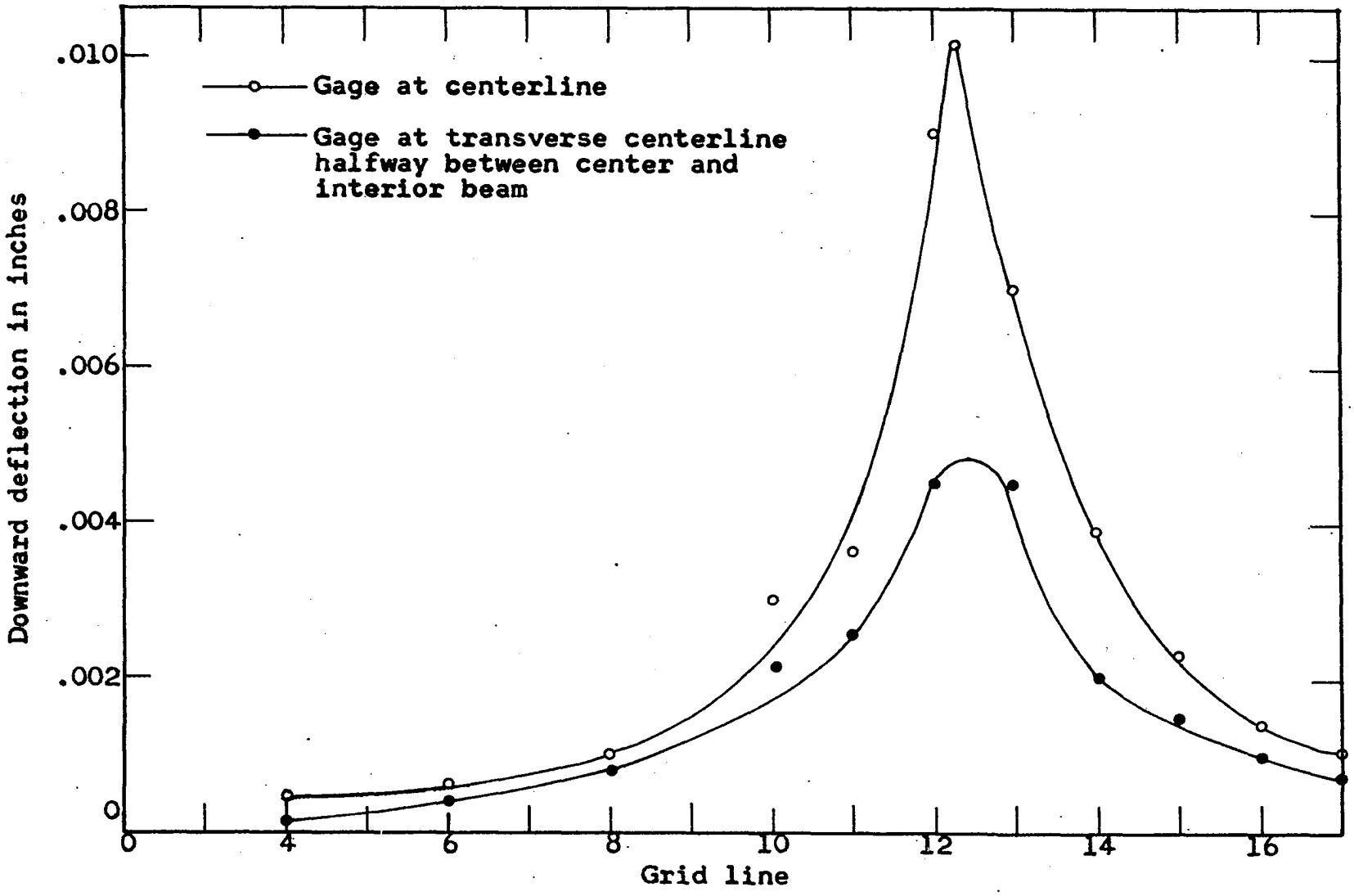

Fig. 5. Influence line for relative deflection of slab at center of 25 foot bridge; 1 kip load moving along longitudinal centerline

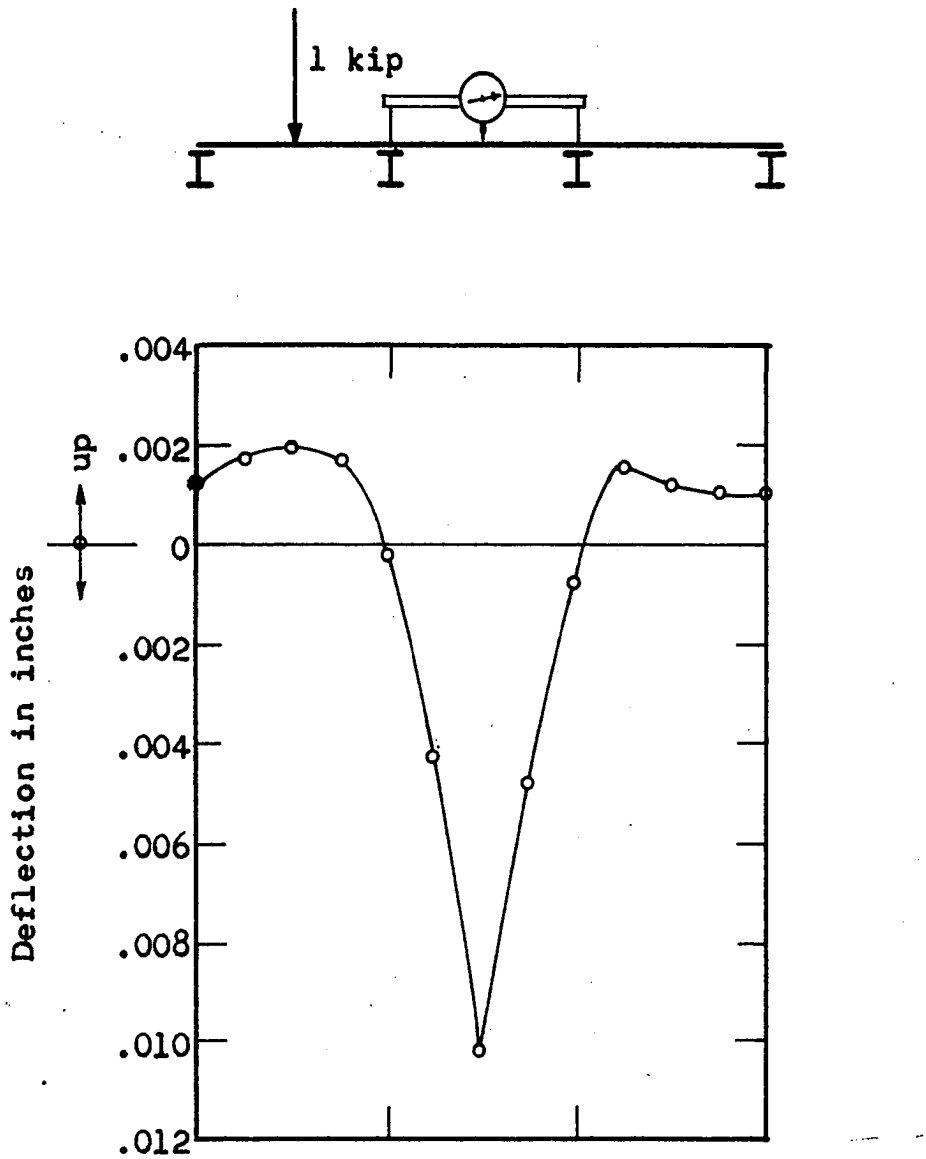

Fig. 6. Influence line for relative deflection of center of slab; 1 kip load moving transversely across bridge at midspan

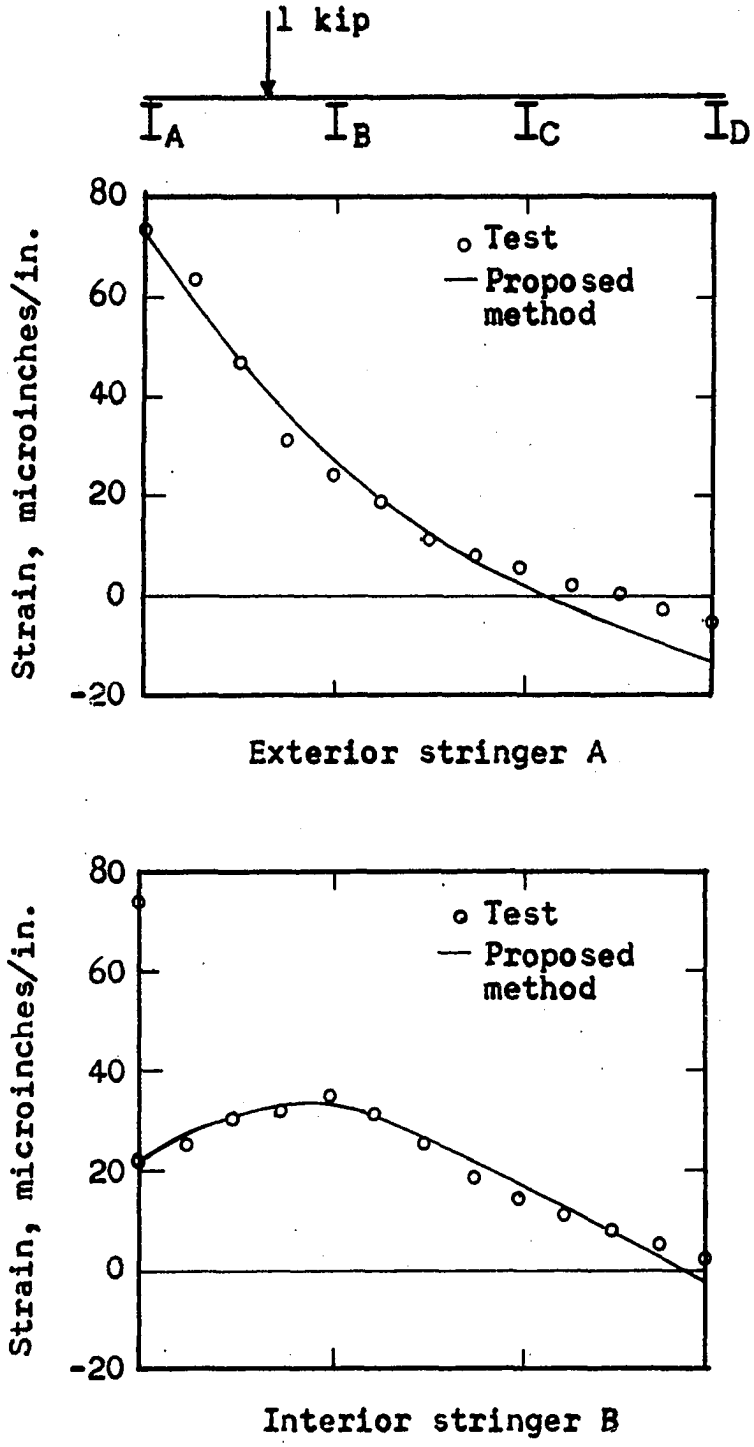

Fig. 7. Influence lines for strain at midspan for stringers in 25 foot bridge; 1 kip load moving along transverse centerline

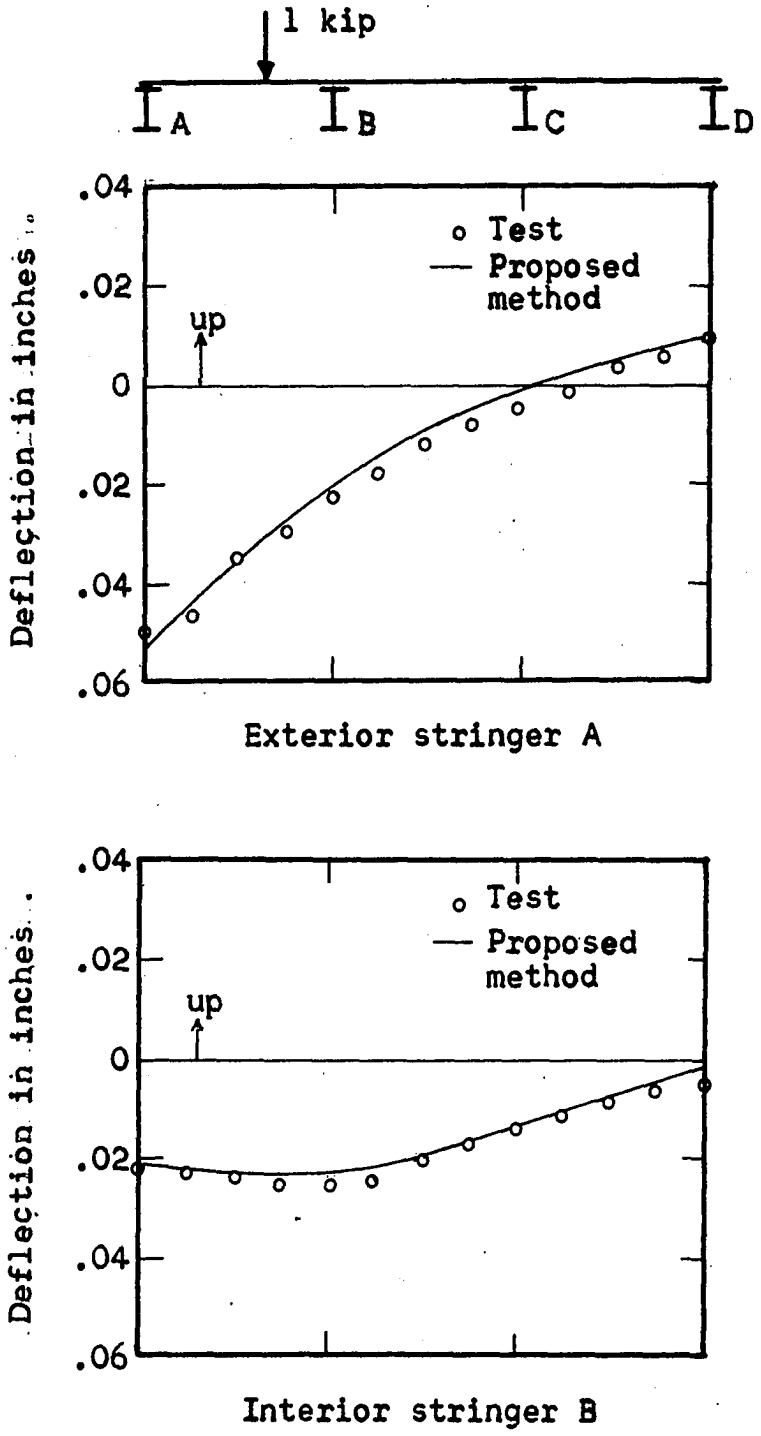

Fig. 8. Influence lines for deflection at midspan for stringers in 25 foot bridge; 1 kip load moving along transverse centerline

the continuous steel stringer bridge was found to be 0.6L. This difference was attributed to the difference in transverse diaphragms for these bridges, the latter two bridges having comparatively light diaphragms at the one-third points.

Tests by Wei (33) have indicated that the effectiveness of diaphragms depends on their position and the stiffness ratio. This stiffness ratio is defined as the dimensionless quantity $r = \frac{EI(diaphragm)}{EI(beam)}$. Thus it can be seen that for small values of r, say less than 0.01, the diaphragms do not contribute much to slab stiffness. Also, diaphragms placed at the one-third points of a span are much less effective than those placed at or very near midspan, since this is the location where maximum moments usually occur. Other factors that influence diaphragm usefulness are the beam spacing to length ratio (S/L) and the ratio of beam to slab stiffness $H = EI/LE_sL$, in which EI is the flexural rigidity of the beam and E_sI_s is the flexural rigidity of the slab per unit width. Thus a high value of H indicates a relatively flexible slab in which a greater percentage of load will be transmitted to individual beams than would be the case with low values of H. It can be seen then that diaphragms would play a much more important role in stiffening bridge floors having high values of H than in the systems having low values. The values of r and H for the bridges tested are tabulated in Tables 1 through 4.

From the examination of the data in Tables 6 through 11, it appears that for bridges with diaphragms at the one-third points, S/L between 0.1 and 0.25 and H not greater than 10, an effective slab width of 0.8L when r is greater than 0.15, and 0.6L when r is less than 0.15 should be used. For three or more diaphragms and similar ratios of S/L and H, an effective slab width of 0.8L is used when r is greater than 0.015, and 0.6L when r is less than 0.015.

In order to show the variation in load distribution for various effective slab widths, Figs. 9 and 10 were drawn, using effective widths of 2.5, 5, 10 and 20 feet for the 25 foot bridge. These graphs show that the change in load distribution decreases as the effective span increases. For example, the maximum percent load variations compared to the total load between the 5 and 10 foot and the 10 and 20 foot width on the 25 foot bridge are 7 percent and 4 percent, respectively. In the bridges tested, the use of 0.6L instead of 0.8L did not cause a variation in maximum loading on beams in any of the test bridges in excess of 8 percent for interior or 6 percent for exterior beams.

The use of such a wide effective slab width does not indicate that there is appreciable longitudinal distribution of the load in the slab itself. Instead, the slab near the load transmits this force directly to the beams through the approximate effective slab width E as used in slab design.

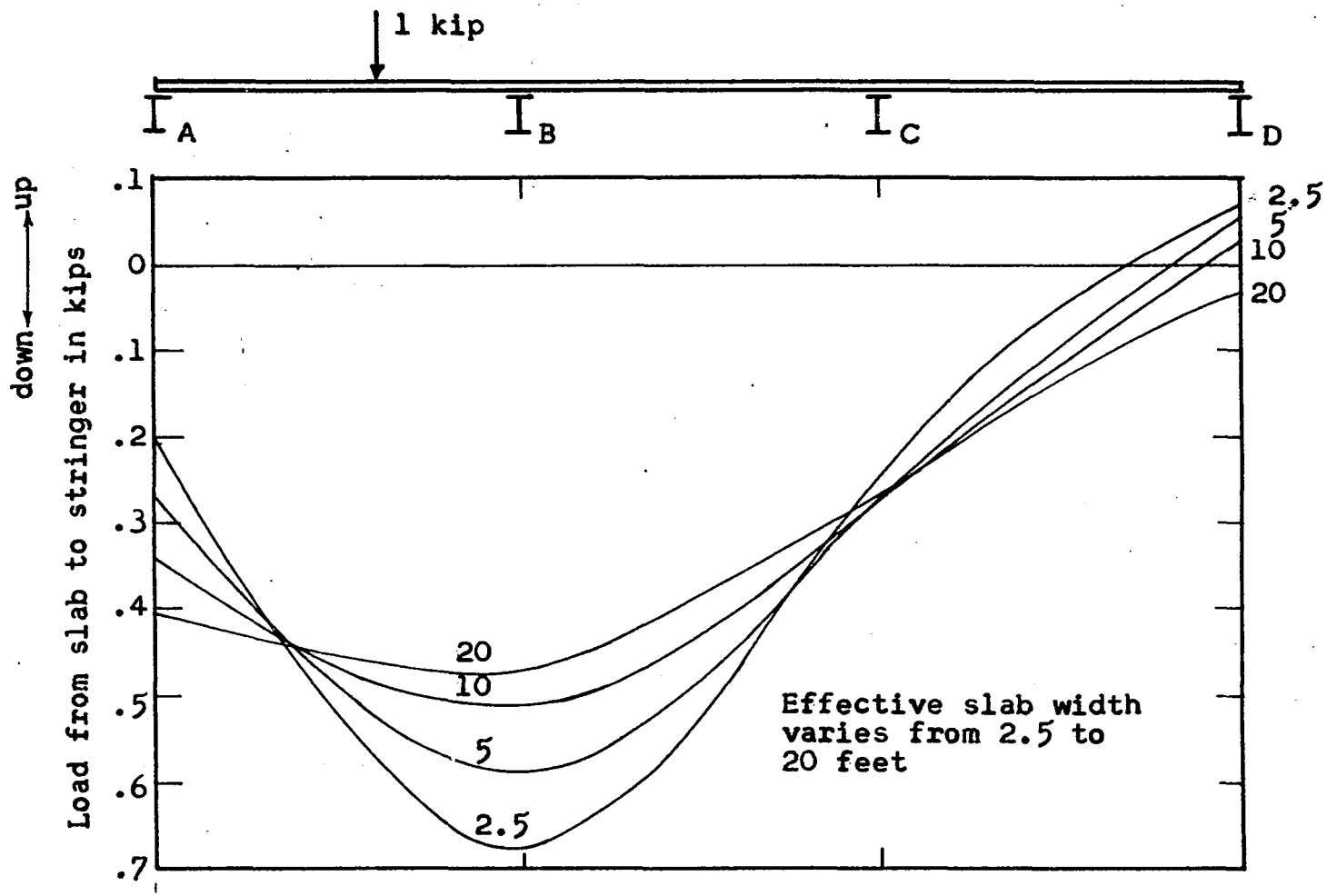

Fig. 9. Influence lines for load to interior stringer B for various effective slab widths at midspan; unit load moving along transverse centerline of 25 foot bridge

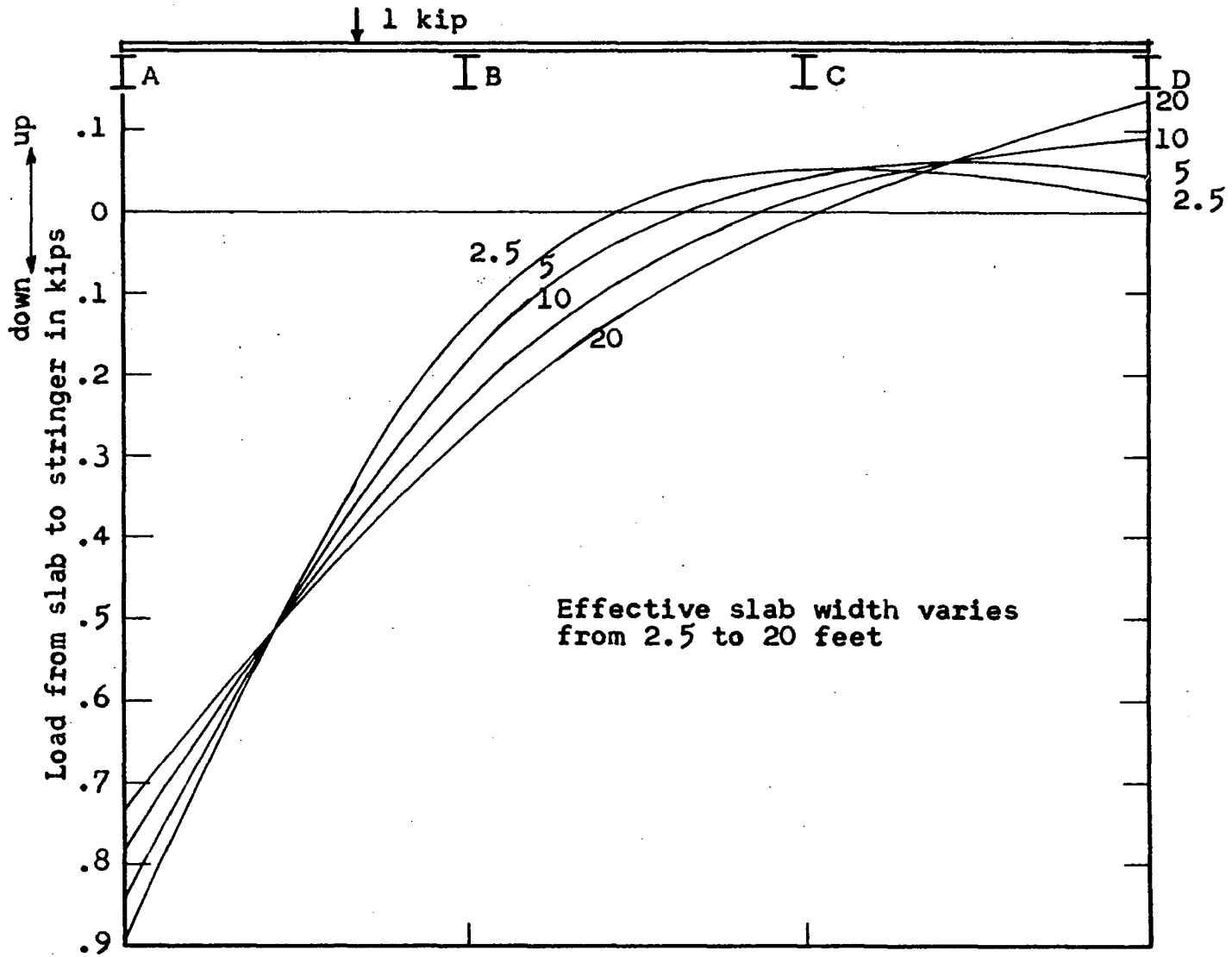

Fig. 10. Influence lines for load to exterior stringer A at midspan; unit load moving along transverse centerline of 25 foot bridge

This load causes the beams to deflect, forcing the slab to deflect longitudinally with it and thus distribute the load over a wider width than E.

Moment Diagrams and Shear Distribution

The shape of the moment diagrams for the interior and exterior stringers of the 25 foot laboratory bridge was determined experimentally using the strain readings measured along these stringers. These values have been plotted (Figs. 11, 12) for both stringers, using loads at midspan and near the one-quarter point. The calculated values, using the equations in Fig. 1 are also plotted, assuming a concentrated reaction acting between the beam and slab. It can be seen that when the load is directly over the beam, the sides of the moment diagram are concave upward, indicating that the slab is exerting an upward force along the beam except in the vicinity of the loading. In this case the calculated values are slightly lower than the measured values. For loads a short distance from the beam in a transverse direction, the moment diagram is concave downward, which indicates a downward distribution reaction on the beam from the slab. Here the calculated values, assuming a concentrated load, are somewhat higher. Since the bulk of the bending moment in a beam is due to the wheels closest to it, the error in using concentrated reactions appears to be small. The calculated values in Figs. 7, 8, 11, 12, and in Tables 6 through 11, were

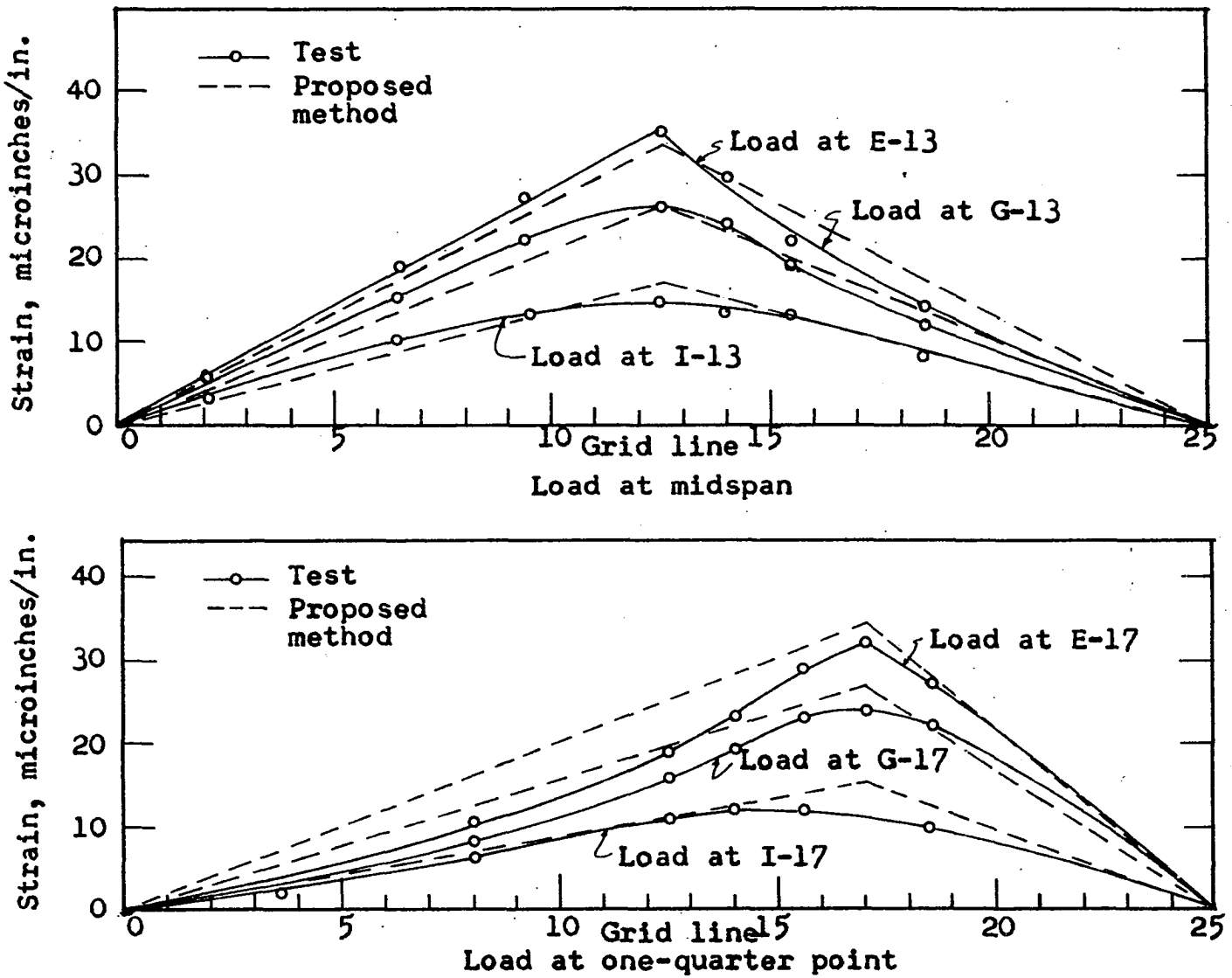

Fig. 11. Strains along interior stringer B for concentrated load of 1 kip; 25 foot bridge

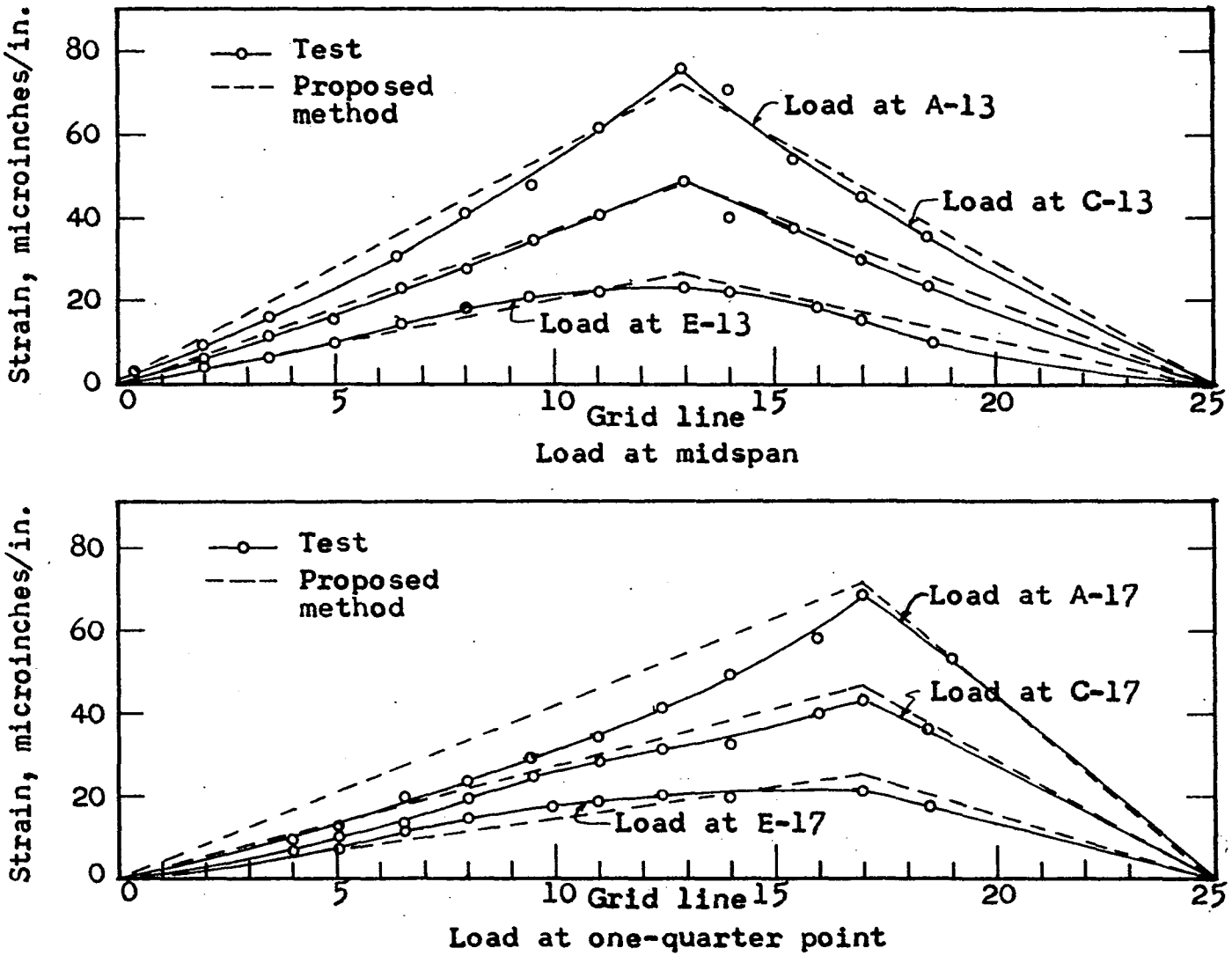

Fig. 12. Strains along exterior stringer A for concentrated load of 1 kip; 25 foot bridge

were obtained in this manner.

If greater accuracy should be desired, different distributions could be used for the more distant loadings, say those beyond a distance of S from the stringer. Several different distributions were tried, assuming two loads of equal magnitude spaced at a distance S at midspan. A comparison of the bending moments at the center of a simply supported stringer, using different assumed load distributions, is shown in Table 5.

Table 5. Maximum moments in stringers for a distributed load

Total distributed load R	Moment at midspan
Concentrated load	RL/4
Uniform load	RL/8
Triangular load (peak at midspan)	RL/6
Sinusoidal load	$RL/2\pi = RL/6.28$

The sinusoidal distribution of the form $p' = p \sin\frac{\pi x}{L}$, where p is the load intensity at midspan, is usually considered the one that most closely approximates the actual distribution of the reactions between beam and slab for distant loadings.

As an example, consider two unit loads on the 25 foot bridge at midspan, directly above the interior stringers. The moment induced in one of the stringers due to both loads can be determined by superposition. These moments when calculated,

assuming a concentrated load, are 6 percent greater than the test results; while the calculated values, assuming that the distant load is sinusoidal in nature, are 7 percent below test figures. For more distant loads the sinusoidal loading approaches the true load; but since these loads have a smaller effect on the total moment, the error in using concentrated loads usually decreases.

The variation of shear in the slab along the edges of the stringers was also studied. Examination of the shear diagrams for the 25 foot laboratory bridge revealed that the maximum shear in the slab at midspan occurs along the inside face of the exterior beam and outside face of the interior beam when loaded with a roving concentrated load. Figs. 13 and 14 show the influence lines calculated by the equations in Fig. 1 for these points at midspan and at the end of the bridge. These diagrams indicate that the maximum shear at midspan is about 70 percent of the maximum shear at the supports. At present AASHO specifications (2, p. 25) state that slabs designed for bending moments in accordance with specifications are to be considered satisfactory in bond and shear. Although this may work satisfactorily for most highway bridges, high shears may be encountered if thin slabs are used. The computation of shear by the proposed method (equations, Fig. 1) would give designers a method of varying bar sizes to meet bond requirements between midspan and the ends of the bridge.

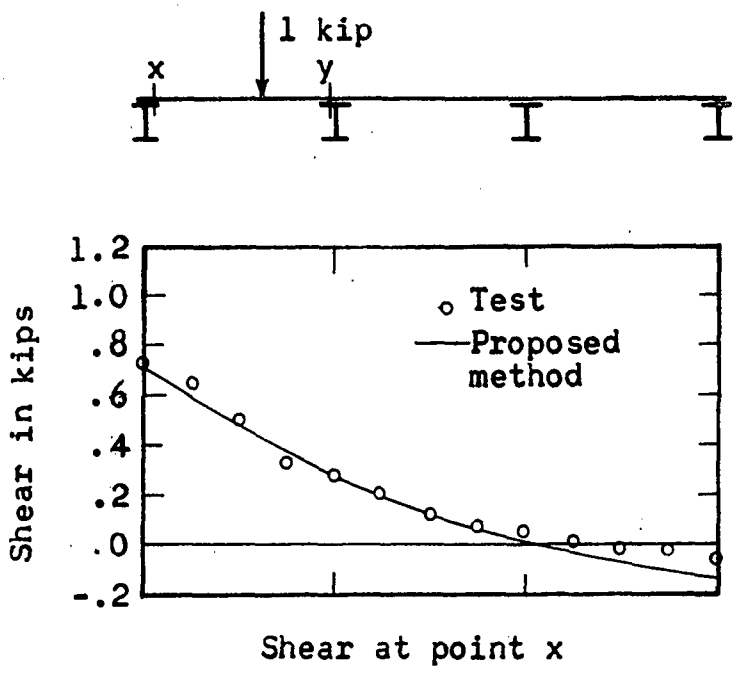

Fig. 13. Influence lines at midspan for shear in the slab; 1 kip concentrated load moving transversely across 25 foot bridge at midspan

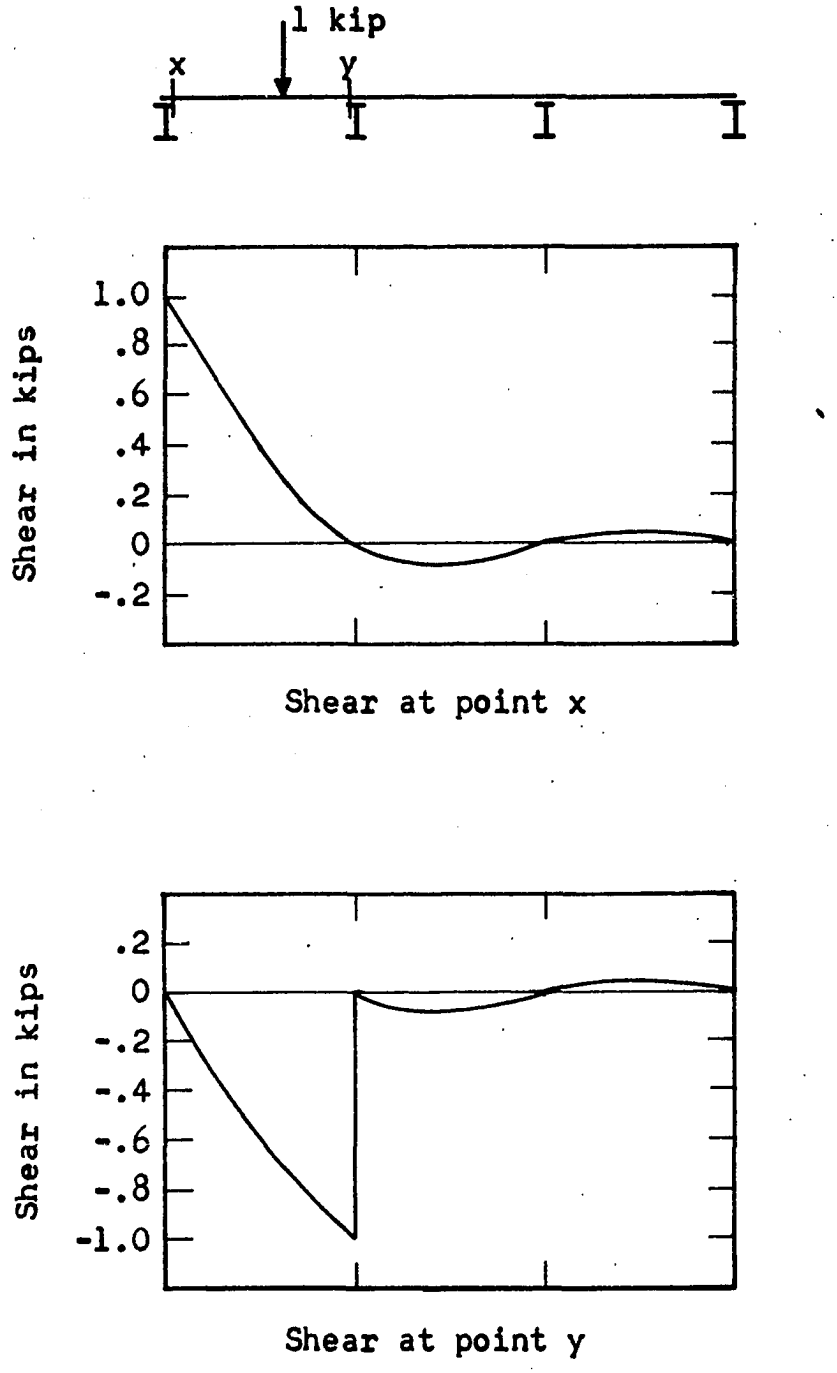

Fig. 14. Influence lines at abutment for shear in the slab; 1 kip concentrated load moving transversely across 25 foot bridge at abutment

Comparison of Predicted and Test Results

The final criterion in developing a practical method of analysis is whether or not it works. In order to decide this, one must determine how much error is allowable and over what range of values it will work satisfactorily. For this purpose Tables 6 through 11 have been prepared. Tables 6 through 9 compare the computed strains in the four simple span bridges with the experimental values. Unfortunately the strain data taken for the continuous bridge was not available but, as

Table 6. Comparison of maximum measured and computed strains in stringers at midspan, using truck loadings, for 10 foot simple span laboratory bridge

	One 4,000 lb axle Wheels 2 ft c-c		Two 4,000 lb axles Trucks 3.33 ft c-c	
	Int. beam	Ext. beam	Int. beam	Ext. beam
	(Strains in microin./in.)			
Observed values[a] by author	270	262	418	312
Observed values by Holcomb	262	255	412	306
Calculated values by author	294	295	443	317
Percent error[b]	9	12	6	2
AASHO 1957	338	466	429	466
Percent error[b]	25	40	3	33

[a]Superposition of concentrated loads to give wheel loads

[b]Percent error is based on observed values taken by author

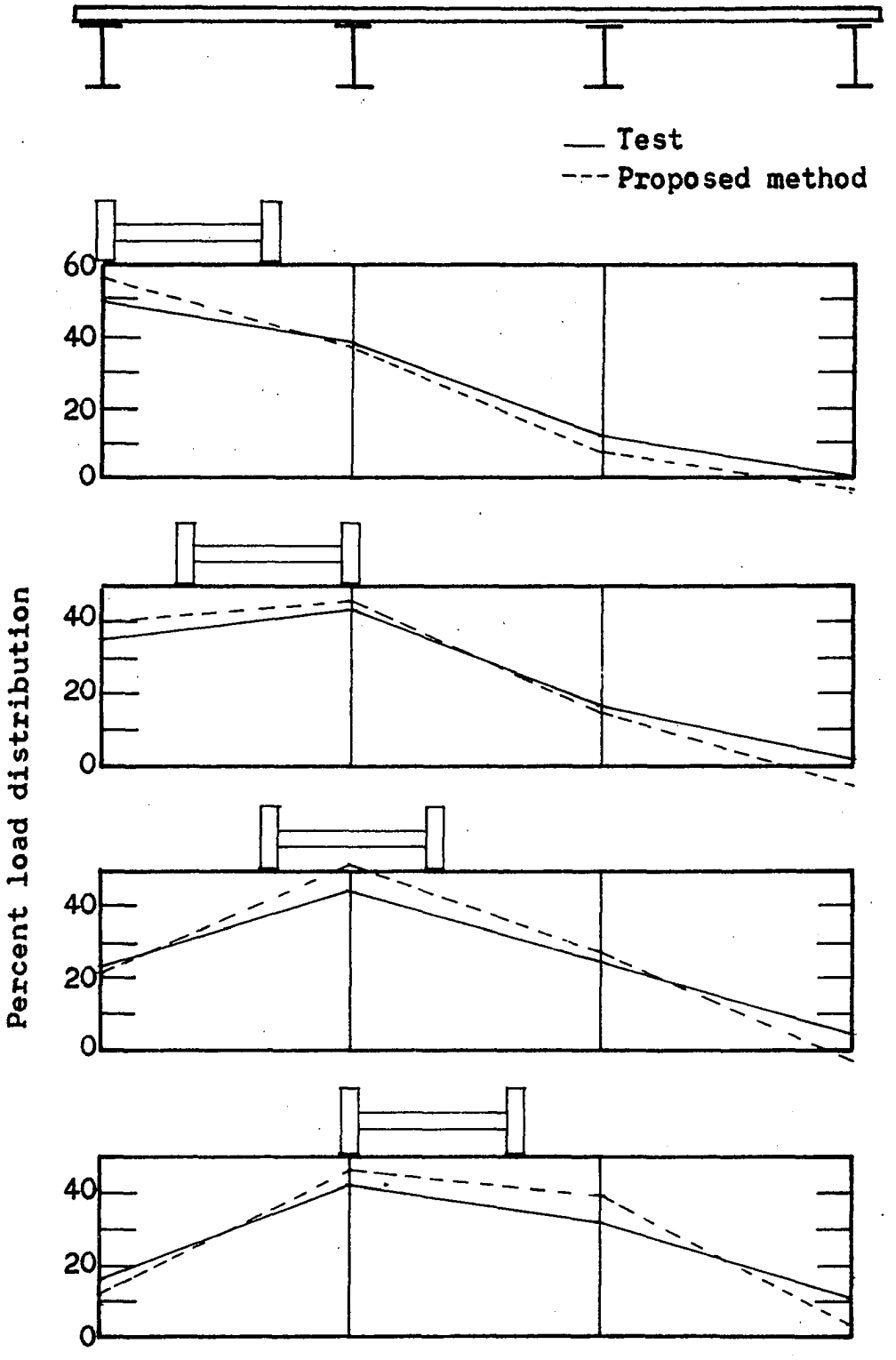

Fig. 15. Static load distribution to stringers for continuous aluminum bridge in outer span at 0.4 of the span from abutment

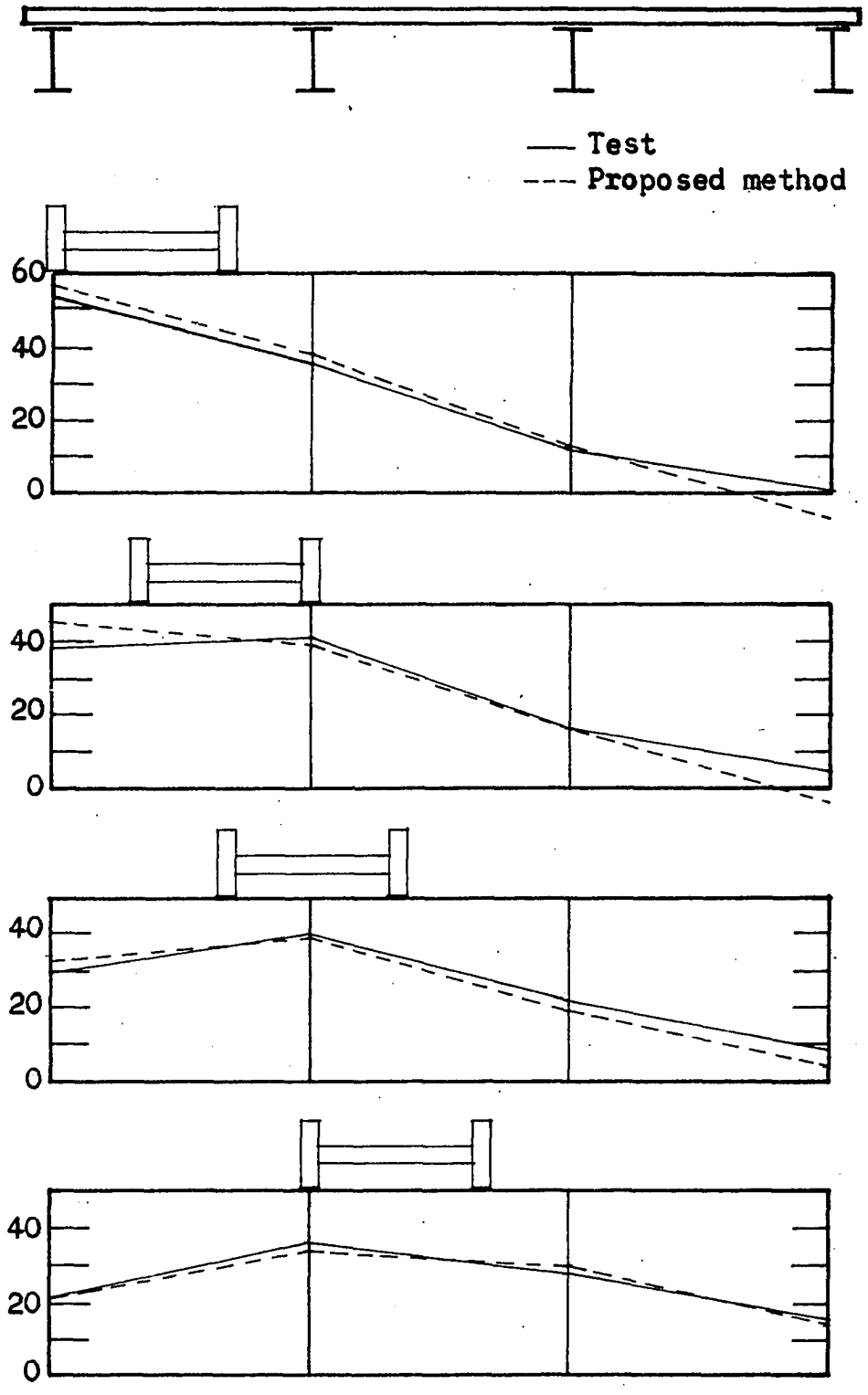

Fig. 16. Static load distribution to stringers for continuous aluminum bridge at midspan of inner span

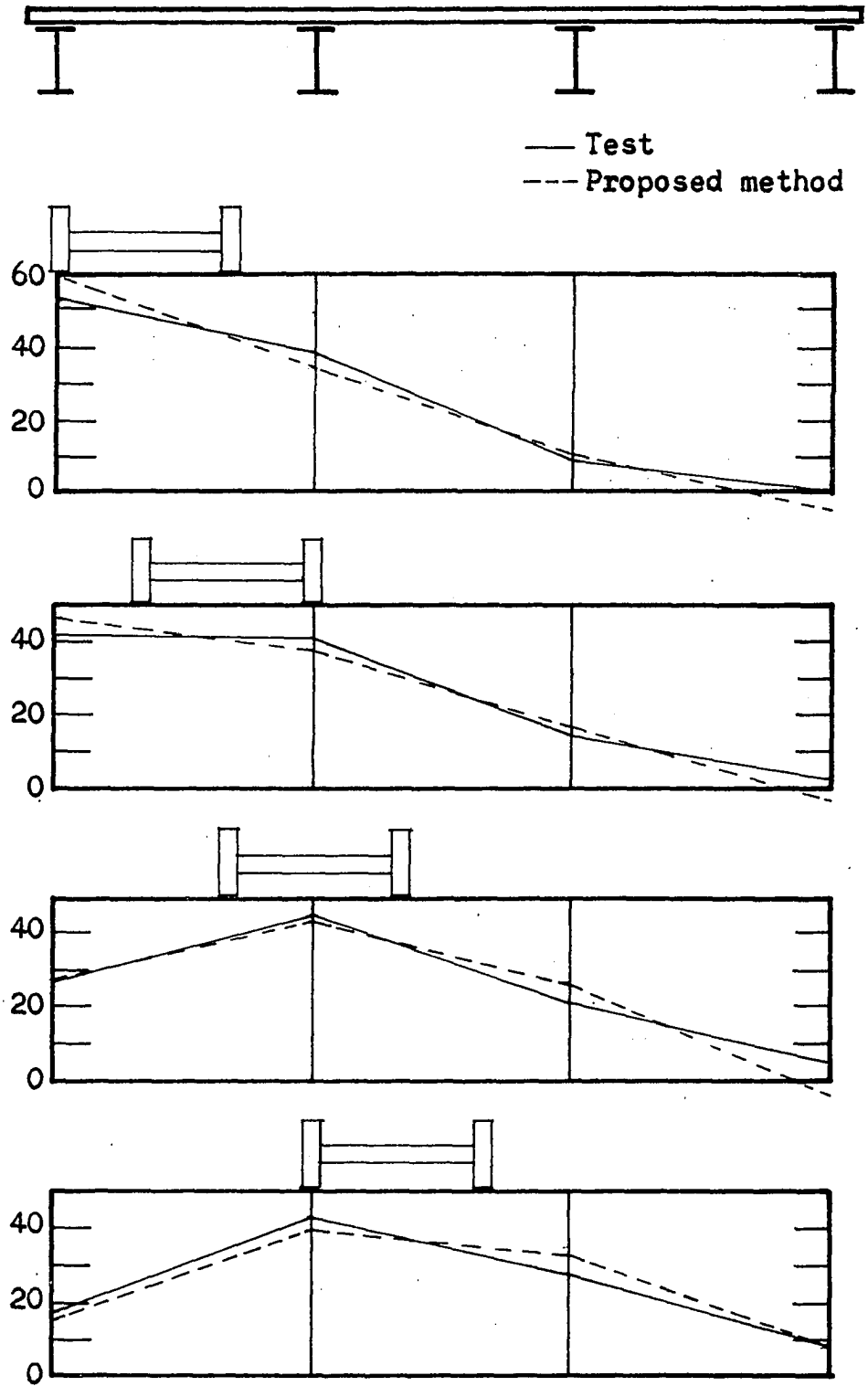

Fig. 17. Static load distribution to stringers of continuous span steel stringer bridge at 0.4 of the span from abutments

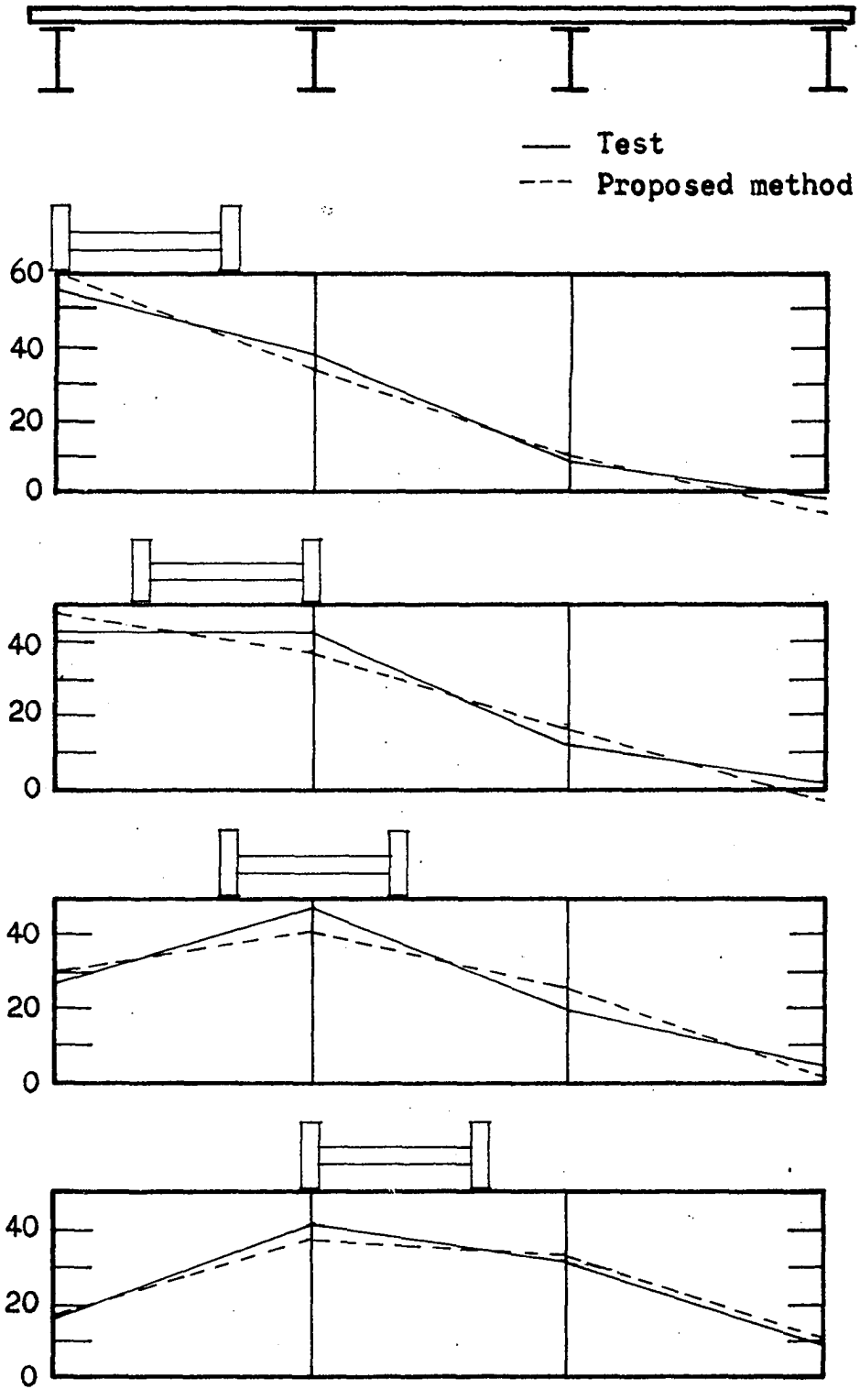

Fig. 18. Static load distribution to stringers for continuous steel stringer bridge at midspan of inner span

previously mentioned, diagrams showing the experimental static load distribution to stringers were drawn by Linger (17). These values have been plotted in Figs. 15, 16, 17, and 18 for various positions of the truck, together with the computed values. The maximum values at the one-quarter point for the outer spans and at midspan for the inner spans are tabulated and compared with the computed values in Tables 10 and 11. In all cases the percent error shown is equal to:

$$\frac{\text{computed value - test value}}{\text{test value}} \times 100 \ .$$

Thus a positive error indicates that the computed value is conservative.

AASHO (2, p. 10) specifies that the position of two trucks side by side should be 10 feet center to center, with the center of the outermost wheel group not less than 2 feet from the inside face of the curb (one-third of these values of course being used for the laboratory bridges). Therefore, only loadings falling within these specified positions are considered in Tables 6 through 11.

An examination of the percent errors between theory and test show that they vary from +12 to -6 percent. The average positive error is 6.0 percent and the average negative error 2.4 percent. The largest positive errors were found to exist in the 10 foot bridge. This is probably due to its short length, which would allow some of the slab to distribute load directly to the abutments.

Table 7. Comparison of maximum measured and computed strains in stringers at midspan, using truck loadings, for 25 foot simple span bridge

	One 4,000 lb axle Wheels 2 ft c-c		Two 4,000 lb axles Trucks 3.33 ft c-c	
	Int. beam	Ext. beam	Int. beam	Ext. beam
	(Strains in microin./in.)			
Observed values[a] by author	130	199	225	243
Observed values by Holcomb	136	192	228	225
Calculated values by author	128	207	230	258
Percent error[b]	-2	4	2	6
AASHO 1957	202	272	257	347
Percent error[b]	47	37	14	39

[a]Superposition of concentrated loads to give wheel loads

[b]Percent error is based on observed values taken by author

Tables 6 through 11 also show values obtained using the 1957 AASHO specifications. The maximum error in this case was 81 percent, the average being 32.7 percent. All these errors were positive, indicating that the AASHO specifications are necessarily conservative. It it also interesting to note that the AASHO specifications show a maximum error of 30 percent and an average error of only 16 percent for the continuous bridges. This probably reflects the use of the later specifications, while the simple span bridges were designed using

Table 8. Comparison of maximum measured and computed strains in stringers at midspan, using truck loadings, for 41.25 foot simple span bridge

	One 33,000 lb truck Wheels 6 ft c-c		Two 33,000 lb trucks Trucks 10 ft c-c	
	Int. beam	Ext. beam	Int. beam	Ext. beam
	(Strains in microin./in.)			
Observed values by Holcomb	236	307	382	351
Calculated values by author	220	328	370	375
Percent error[a]	-6	4	-3	5
AASHO 1957	315	493	400	628
Percent error[a]	34	60	5	79

[a]Percent error based on observed values taken by Holcomb

earlier load distribution formulas.

The above comparisons indicate that the proposed method, while somewhat more involved, is certainly more accurate than the present AASHO specifications used in designing highway bridge floors.

Use of the Proposed Load Distribution Method

In order to use the reaction values from slab to beam for practical bridge design, the concentrated loads must be superimposed to obtain wheel loads, uniform lane and line loads. To check the validity of superposition, test loads on the 10

Table 9. Comparison of maximum measured and computed strains in stringers at midspan, using truck loadings, for 71.25 foot simple span bridge

	One 59,000 lb truck Wheels 6 ft c-c		Two 59,000 lb trucks Trucks 10 ft c-c	
	Int. beam	Ext. beam	Int. beam	Ext. beam
	(Strains in microin./in.)			
Observed values by Holcomb	165	250	285	318
Calculated values by author	172	264	307	314
Percent error[a]	4	6	8	-1
AASHO 1957	264	452	336	575
Percent error[a]	60	81	18	81

[a]Percent error is based on observed values taken by Holcomb

and 25 foot bridges were combined to obtain truck loading and were compared with Holcomb's results, using truck loads. These were reasonably close when checked (Tables 6 and 7).

The procedure, then, for practical design would be as follows:

1. Using the program which has been worked out for the 650 Computer, data cards can be punched for the various parameters of the bridge. These are length of bridge, spacing of stringers, EI of slab and beams, and the various coordinates of load position. The computer can solve these at the rate of one solution every six seconds, solving about 400 problems in

Table 10. Comparison of wheel load distribution to stringers at midspan, using truck loadings, for 220 foot four span continuous aluminum stringer bridge

	Two H-20 trucks Trucks 10 ft c-c		Two H-20 trucks Trucks 10 ft c-c	
	Outer span		Inner span	
	Int. beam	Ext. beam	Int. beam	Ext. beam
	(Fraction of wheel load)			
Observed values by Linger	1.62	1.14	1.41	1.31
Calculated values by author	1.71	1.23	1.42	1.41
Percent error[a]	6	8	1	8
AASHO 1957	1.73	1.49	1.73	1.49
Percent error[a]	7	30	23	14

[a]Percent error is based on observed values taken by Linger

approximately 40 minutes. If the bridge is symmetrical, it is necessary to solve only one-fourth of the total bridge. The size of the grid is optional; however, enough points should be taken so that interpolation between points should not be necessary. A 2 x 2 grid should be satisfactory for a full-sized bridge; or if desired, only those points that correspond to the wheel positions need to be solved. It should also be noted that usually only the center portion of the bridge need be solved, since the moments due to loads near the ends of the bridge are never maximum unless there are unusual loading

Table 11. Comparison of maximum wheel load distribution to stringers at midspan, using truck loadings, for 240 foot four span continuous steel bridge

	Two H-20 trucks Trucks 10 ft c-c		Two H-20 trucks Trucks 10 ft c-c	
	Outer span		Inner span	
	Int. beam	Ext. beam	Int. beam	Ext. beam
	(Fraction of wheel load)			
Observed values by Linger	1.52	1.20	1.48	1.24
Calculated values by author	1.44	1.30	1.42	1.32
Percent error[a]	-5	8	-4	6
AASHO 1957	1.64	1.44	1.64	1.44
Percent error[a]	8	20	11	16

[a]Percent error is based on observed values taken by Linger

conditions.

2. The reaction from slab to any stringer can be obtained by combining all values that correspond to the truck wheel positions.

3. The bending moments in the stringers can be obtained by solving for the moments due to the concentrated reaction acting on the stringer; or the moments of the more distant wheels can be found by working out separately the bending moments, using distributed load formulas similar to those in Table 5 and then combined to give the final moment.

4. Uniform loads such as dead load and lane loads can be obtained by adding the reactions due to a line of concentrated loads across the bridge. This gives the uniform load per unit grid width from which the bending moment for a uniform load can be obtained. The reaction to a beam varies very little as the line load moves longitudinally along the bridge, the greatest variation being near the ends as shown in Fig. 19. Since the loads at the end of the beam do not appreciably affect the maximum bending moment, a value of reaction for the line load near the center can be used as an average uniform load. It should be noted that the values in Fig. 19 represent the type of loading a stringer would have if the bridge were loaded with a uniform load over its entire roadway. It can be seen that for the 25 foot bridge near mid-span, a uniform load on the slab is divided to each stringer very nearly in proportion to the distance half-way between stringers. However, for the continuous steel stringer bridge, which has exterior stringers of greater stiffness than interior stringers (the only case in all the bridges tested), the uniform load carried by the exterior stringers is 30 percent greater and that for the interior stringers 17 percent less than the amount based on stringer spacing. Thus it can be seen that considerable error may result when relative stringer stiffness is not considered in designing for uniform loading.

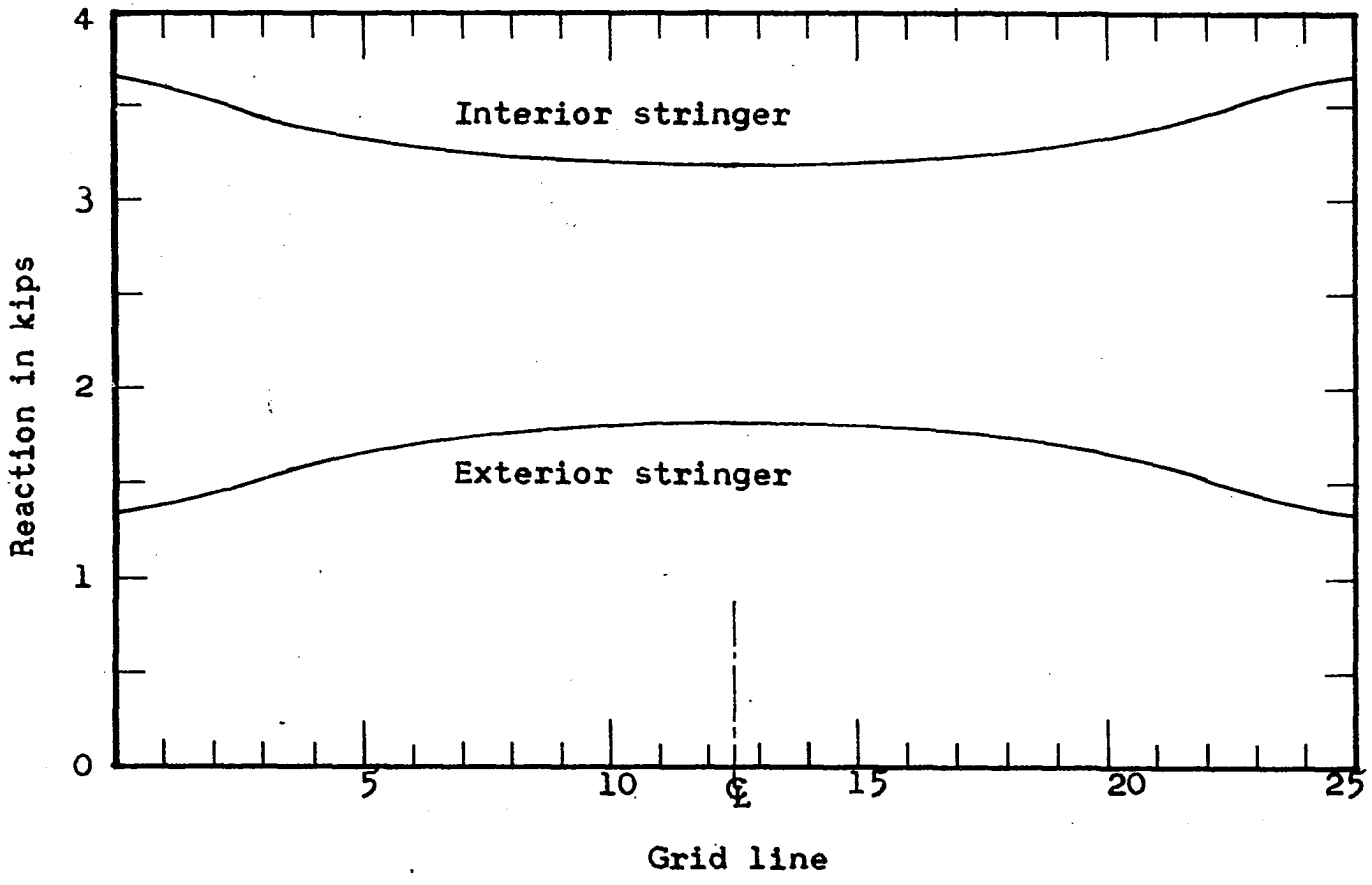

Fig. 19. Slab to stringer reactions; transverse uniform line load of 1 kip/foot moving longitudinally along the 25 foot bridge

Limitations of the Equations

The equations are based on the assumption that most of the reinforcement is transverse. In short bridges with considerable longitudinal reinforcement, much of the load would be distributed to the end reactions, and the solutions could be used only as a rough guide.

Also, the equations are derived, assuming both that the slab is uniform in thickness and that the stringer sizes are symmetrical. If the stringers have variable moments of inertia, the equations have to be modified. This could be done easily if the variation is in some form easily integrated, such as the reciprocal I form. The formulas also do not take into consideration an overhang of slab on the exterior beam; however, this could be taken into account by a simple modification.

Since the equations are solved for a four stringer bridge, they are not applicable to a bridge with a greater number. Five and six beam solutions, while more involved, could be worked out.

The method is derived assuming simple span bridges. However, the continuous bridges checked showed that the load distribution is not appreciably different than that for simple span bridges. When investigating continuous bridges, it might seem more logical to use the span length as the distance between inflection points on the bridge, since this would

correspond to a simple span. However, comparison of the method with test results indicates that this refinement is not necessary. The equations have been derived, assuming the general case in which each stringer could have a different stiffness. While most bridges are symmetrical, it is possible that unusual conditions might result in a design using a non-symmetrical arrangement of stringers. If such were the case, the equations in the proposed method should give much better results than the standard AASHO specifications.

As stated previously, the equations have been derived, neglecting the effect of torsion in the girders on load distribution. This assumption is justified as long as the beams are wide flange sections, since they have very little resistance to twisting. Also, the results of the tests seem to verify this assumption. When concrete beams are used, however, either conventional reinforced or prestressed, it may not be possible to ignore completely this effect. Tests run by Mattock and Kaar (19) on a reinforced concrete slab rigidly connected to prestressed concrete girders showed a decrease in deflection of exterior beams by about 20 percent, and interior beams 10 percent. This of course would indicate a considerable change in load distribution. This could be taken into account in the proposed method by including the energy expression for torsion as well as moment. An approximate method for taking torsion into account would be to add the torsional stiffness of the beam, say at midspan, to the

flexural stiffness of the slab, using the effective width E. Since both slab and stringer must rotate through the same angle, the approximate equivalent stiffness at midspan would be $\frac{4EI}{L} + \frac{4KG}{L}$, where EI is the flexural rigidity of the slab, G the shearing modulus, and K an expression roughly the equivalent of the polar moment of inertia for rectangular or tee-shaped sections. In practice, KG is usually evaluated by fixing one end of a beam, rotating the other end using a known torque and measuring the angle of twist. Once the equivalent stiffness is determined, the total effective slab width could be increased by this amount and the problem treated as before. Such a method should work as long as the torsional stiffness is not too large in proportion to the slab stiffness. At any rate, such a procedure should be checked by tests in order to determine these limits.

CONCLUSIONS AND RECOMMENDATIONS

Examination of the results obtained from these tests in connection with load distribution in beam and slab bridge floors has led to the following conclusions:

1. The result of the computed load distribution compares favorably with the test data obtained from the six bridges investigated. This indicates that the method is applicable for stringer to slab stiffness (H) values between 3 and 10, and stringer spacing to length ratios (S/L) from 0.13 to 0.32, these being the limits of the bridges tested. However, there seems to be no reason why the method should not apply for H values as low as 2 and as high as 20. The only limiting factor is that for low values of H, the slab may transmit some of its load directly to the abutments.

2. The proposed method seems to work satisfactorily for continuous bridges as well as simple span bridges.

3. The present AASHO specifications, while better than those prior to 1957, are still conservative and limited to stereotyped bridge floors.

4. Diaphragms can be taken into account by considering their rigidity as part of the slab stiffness. The effective width of the slab can be varied in accordance with the limitations outlined on page 50. In general, conventional diaphragms

can be taken into account by increasing the effective width of slab by about 0.2 of the bridge span.

5. Torsion effects can be neglected in bridge floors using conventional I-beams to support reinforced concrete slabs. However, this evidently is not the case for monolithic slab and concrete beam systems. A simple method, such as that suggested on page 74, should be devised to handle these systems.

6. Use of the proposed method is not practical without access to an electronic computer, since the solutions are too lengthy by manual methods. However, computers are now in common enough use tha even small consulting firms can have the computing done by an office owning or leasing computers. It would also be possible, if the demand were large enough, to solve a large number of bridge floors in dimensionless form, including the various parameters of stringer spacings, span lengths, and ratios of slab and beam stiffness. This data could then be combined in the form of graphs or tables, from which the load distribution values could be obtained. With such a set of graphs, any engineer versed in bridge structures could design a floor system more economical and in some cases safer than the method recommended by present AASHO specifications.

BIBLIOGRAPHY

1. Agg, T. R. and Nichols, C. S. Load concentrations on steel floor joists of wood floor highway bridges. Iowa State College Eng. Expt. Sta. Bulletin 53. 1919.

2. American Association of State Highway Officials. Standard specifications for highway bridges. 7th ed. Washington, the Association. 1957.

3. Clough, R. W. and Scheffey, C. F. Stress measurements San Leandro Creek bridge. Trans. Am. Soc. of Civil Eng. 120: 939-954. 1955.

4. Foster, G. M. Test on rolled-beam bridge using H20-S16 loading. Highway Res. Bd. Res. Rep. 14-B: 10-38. 1952.

5. Fuller, A. H. Preliminary impact studies--Skunk River bridge on the Lincoln Highway near Ames, Iowa. Iowa State College Eng. Expt. Sta. Bulletin 63. 1922.

6. _____ Effect of trucks upon a few bridge floors in Iowa in 1922 and in 1948. Highway Res. Bd. Res. Rep. 14-B: 1-9. 1952.

7. _____ Skunk River bridge exhibits composite action after twenty-eight years of service. Civil Eng. 21: 400-402. 1951.

8. _____ Skunk River bridge exhibits composite action after twenty-eight years of service. Iowa State College Eng. Expt. Sta. Eng. Rep. 9: 21-24. 1952.

9. _____ and Caughey, R. A. Experimental impact studies on highway bridges. Iowa State College Eng. Expt. Sta. Bulletin 75. 1925.

10. Gossard, M. L., Siess, C. P., Newmark, N. M., and Goodman, L. E. Studies of highway skew slab bridges with curbs. University of Illinois Eng. Expt. Sta. Bulletin 386. 1950.

11. Guyon, Y. Calcul des ponts large à poutres multiples solidarisés par des entretoises. Annales des Ponts et Chaussées, Paris 116: 553-612. 1946.

12. Holcomb, R. M. Distribution of loads in beam and slab bridges. Unpublished Ph.D. Thesis. Ames, Iowa, Library, Iowa State University of Science and Technology. 1956.

13. _____ Distribution of loads in beam and slab bridges. Iowa Highway Res. Bd. Bulletin 12. 1956.

14. Holl, D. L. Analysis of thin rectangular plates supported on opposite edges. Iowa State College Eng. Expt. Sta. Bulletin 129. 1936.

15. Jensen, V. P. Solutions for certain rectangular slabs continuous over flexible supports. University of Illinois Eng. Expt. Sta. Bulletin 303. 1938.

16. Lin, T. Y. and Horonjeff, R. Load distribution between girders on San Leandro Creek bridges. Highway Res. Bd. Res. Rep. 14-B: 39-45. 1952.

17. Linger, D. A. and Hulsbos, C. L. Dynamics of highway bridges. Iowa State University Eng. Expt. Sta. Bulletin 188. 1960.

18. Massonnet, C. Méthode de calcul des ponts à poutres multiple tenant compte de leur résistance à la torsion. Publications, International Association for Bridge and Structural Engineering, Zurich 10: 147-182. 1950.

19. Mattock, A. H. and Kaar, P. H. Precast-prestressed concrete bridges. Journal of the Research Laboratories, Portland Cement Assn. 3, No. 3: 30-70. 1961.

20. Newmark, N. M. Design of I-beam bridges. Trans. Am. Soc. of Civil Eng. 114: 997-1022. 1949.

21. _____ Design of I-beam bridges. University of Illinois Eng. Expt. Sta. Reprint 45. 1949.

22. _____ A distribution procedure for the analysis of slabs continuous over flexible beams. University of Illinois Eng. Expt. Sta. Bulletin 304. 1938.

23. _____ and Siess, C. P. Design of slab and stringer highway bridges. Public Roads 23: 157-164. 1943.

24. _____ _____ Moments in I-beam bridges. University of Illinois Eng. Expt. Sta. Bulletin 336. 1942.

25. _____ _____ Research on highway bridge floors. Proc. Highway Res. Bd. 33: 30-53. 1954.

26. _____ _____ Research on highway bridge floors. University of Illinois Eng. Expt. Sta. Reprint 52. 1954.

27. _____ _____ and Penman, R. R. Studies of slab and beam highway bridges, Part I. University of Illinois Eng. Expt. Sta. Bulletin 363. 1946.

28. Parcel, J. I. and Maney, C. A. Statically indeterminate structures. 2nd ed. New York, John Wiley and Sons, Inc. 1936.

29. Richart, F. E. and Kluge, R. W. Tests of reinforced concrete slab subjected to concentrated loads. University of Illinois Eng. Expt. Sta. Bulletin 314. 1939.

30. Siess, C. P. and Veletsos, A. S. Distribution of loads to girders in slab and girder bridges: theoretical analyses and their relation to field tests. Highway Res. Bulletin 14-B. 1952.

31. Spangler, M. G. Distribution of end reactions of concrete floor slabs under concentrated loads. Proc. Highway Res. Bd. 32: 144-160. 1953.

32. _____ The distribution of shearing stresses in concrete floor slabs under concentrated loads. Iowa State College Eng. Expt. Sta. Bulletin 126. 1936.

33. Wei, B. C. F. Load distribution of diaphragms in I-beam bridges. Struc. Div., Proc. of Am. Soc. of Civil Eng. 85, No. ST5: 17-55. 1959.

34. Westergaard, H. M. Computation of stresses in bridge slabs due to wheel loads. Public Roads 11: 1-23. 1930.

35. _____ and Slater, W. A. Moments and stresses in slabs. Proc. Am. Conc. Inst. 17: 415-538. 1921.

36. Wise, J. A. Dynamics of highway bridges. Proc. Highway Res. Bd. 32: 180-187. 1953.

ACKNOWLEDGMENTS

The author wishes to express appreciation to the members of his Graduate Committee, Professors R. A. Caughey (Chairman), E. W. Anderson, C. E. Ekberg, Jr., J. J. L. Hinrichsen, Glenn Murphy, and M. G. Spangler, for their patience and instruction throughout the writer's graduate program. He is especially grateful to Professor Caughey for all the time, interest, and many helpful suggestions given.

Acknowledgment is also due the Iowa Highway Research Board, the sponsor of this project; and to Mr. Mark Morris, former Director of Highway Research, whose cooperation made it possible to carry on the experimental work.

APPENDIX

In the following tables some of the slab to beam reaction values have been tabulated for the 25 and 10 foot laboratory bridges. These values have been computed, using the equations in Fig. 1. In order to show the variation in load distribution due to slab stiffness, the values obtained, using two different effective slab widths for each bridge, are listed. The loading used is a unit concentrated load located at the grid points indicated (Fig. 3). A positive sign for the reaction indicates that the load from the slab is acting downward on the beam, while a negative sign indicates an upward force acting on the beam.

Table 12. Influence tables for reactions from slab to beams for single concentrated load. Twenty-five foot bridge

(See Fig. 3, p. 29 for location of grid points)

Position of load (Grid No.) b	a	Effective slab width = 10' R_A	R_B	R_C	R_D	Effective slab width = 20' R_A	R_B	R_C	R_D
0	A	1.0000	0.0000	0.0000	0.0000	1.0000	0.0000	0.0000	0.0000
	B	0.6875	0.3906	-0.0937	0.0156	0.6875	0.3906	-0.0937	0.0156
	C	0.4000	0.7249	-0.1499	0.0249	0.4000	0.7249	-0.1499	0.0249
	D	0.1612	0.9477	-0.1308	0.0218	0.1612	0.9477	-0.1308	0.0218
	E	0.0000	1.0000	0.0000	0.0000	0.0000	1.0000	0.0000	0.0000
	F	-0.0720	0.8517	0.2612	-0.0408	-0.0720	0.8517	0.2612	-0.0408
	G	-0.0750	0.5750	0.5749	-0.0749	-0.0750	0.5750	0.5749	-0.0749
1	A	0.9817	0.0399	-0.0249	0.0033	0.9666	0.0708	-0.0416	0.0041
	B	0.6871	0.3842	-0.0798	0.0085	0.6860	0.3804	-0.0688	0.0024
	C	0.4148	0.6797	-0.1042	0.0095	0.4257	0.6466	-0.0706	-0.0018
	D	0.1861	0.8784	-0.0670	0.0023	0.2050	0.8270	-0.0208	-0.0112
	E	0.0270	0.9290	0.0608	-0.0169	0.0479	0.8758	0.1043	-0.0282
	F	-0.0523	0.8053	0.2947	-0.0477	-0.0363	0.7698	0.3178	-0.0513
	G	-0.0681	0.5680	0.5680	-0.0680	-0.0614	0.5614	0.5614	-0.0614
2	A	0.9460	0.1102	-0.0588	0.0024	0.9123	0.1682	-0.0734	-0.0071
	B	0.6833	0.3772	-0.0544	-0.0060	0.6762	0.3767	-0.0323	-0.0207
	C	0.4386	0.6074	-0.0305	-0.0154	0.4547	0.5573	0.0210	-0.0331
	D	0.2285	0.7649	0.0330	-0.0264	0.2613	0.6825	0.0993	-0.0432
	E	0.0746	0.8109	0.1542	-0.0397	0.1138	0.7226	0.2132	-0.0496
	F	-0.0151	0.7254	0.3429	-0.0532	0.0184	0.6620	0.3688	-0.0493
	G	-0.0511	0.5511	0.5511	-0.0511	-0.0310	0.5310	0.5310	-0.0310

Table 12 (Continued)

Position of load (Grid No.) b	a	Effective slab width = 10' R_A	R_B	R_C	R_D	Effective slab width = 20' R_A	R_B	R_C	R_D
3	A	0.9106	0.1708	-0.0737	-0.0077	0.8648	0.2385	-0.0715	-0.0318
	B	0.6758	0.3769	-0.0312	-0.0214	0.6616	0.3842	-0.0035	-0.0424
	C	0.4553	0.5553	0.0231	-0.0338	0.4694	0.5107	0.0702	-0.0504
	D	0.2627	0.6790	0.1019	-0.0438	0.2980	0.5991	0.1560	-0.0532
	E	0.1156	0.7188	0.2154	-0.0499	0.1613	0.6288	0.2581	-0.0483
	F	0.0201	0.6592	0.3696	-0.0489	0.0637	0.5887	0.3795	-0.0321
	G	-0.0299	0.5299	0.5299	-0.0299	0.0025	0.4974	0.4974	0.0025
4	A	0.8799	0.2172	-0.0744	-0.0228	0.8271	0.2879	-0.0574	-0.0576
	B	0.6667	0.3810	-0.0124	-0.0353	0.6475	0.3947	0.0179	-0.0601
	C	0.4655	0.5231	0.0569	-0.0456	0.4765	0.4871	0.0961	-0.0597
	D	0.2873	0.6223	0.1418	-0.0514	0.3218	0.5511	0.1805	-0.0535
	E	0.1470	0.6555	0.2477	-0.0503	0.1948	0.5714	0.2725	-0.0388
	F	0.0495	0.6104	0.3787	-0.0388	0.0985	0.5395	0.3737	-0.0118
	G	-0.0086	0.5086	0.5086	-0.0086	0.0319	0.4680	0.4680	0.0319
5	A	0.8554	0.2525	-0.0684	-0.0385	0.7984	0.3232	-0.0418	-0.0798
	B	0.6579	0.3868	0.0024	-0.0472	0.6358	0.4044	0.0337	-0.0739
	C	0.4716	0.5033	0.0782	-0.0532	0.4802	0.4742	0.1108	-0.0653
	D	0.3049	0.5846	0.1642	-0.0538	0.3380	0.5215	0.1914	-0.0509
	E	0.1709	0.6118	0.2636	-0.0463	0.2187	0.5342	0.2754	-0.0283
	F	0.0734	0.5745	0.3789	-0.0269	0.1245	0.5053	0.3639	0.0061
	G	0.0104	0.4895	0.4895	0.0104	0.0555	0.4444	0.4444	0.0555

Table 12 (Continued)

Position of load (Grid No.) b	a	Effective slab width = 10' R_A	R_B	R_C	R_D	Effective slab width = 20' R_A	R_B	R_C	R_D
6	A	0.8838	0.2794	-0.0604	-0.0528	0.7769	0.3486	-0.0283	-0.0973
	B	0.6501	0.3926	0.0141	-0.0570	0.6266	0.4123	0.0454	-0.0843
	C	0.4754	0.4907	0.0921	-0.0583	0.4823	0.4665	0.1199	-0.0688
	D	0.3178	0.5587	0.1771	-0.0538	0.3492	0.5020	0.1964	-0.0477
	E	0.1891	0.5808	0.2709	-0.0409	0.2359	0.5089	0.2743	-0.0191
	F	0.0924	0.5478	0.3754	-0.0157	0.1439	0.4811	0.3543	0.0205
	G	0.0266	0.4733	0.4733	0.0266	0.0736	0.4263	0.4263	0.0736
7	A	0.8175	0.2999	-0.0525	-0.0649	0.7610	0.3671	-0.0174	-0.1107
	B	0.6436	0.3978	0.0232	-0.0647	0.6196	0.4185	0.0539	-0.0921
	C	0.4778	0.4824	0.1014	-0.0617	0.4835	0.4617	0.1257	-0.0711
	D	0.3274	0.5406	0.1848	-0.0529	0.3573	0.4888	0.1987	-0.0449
	E	0.2029	0.5584	0.2741	-0.0355	0.2484	0.4912	0.2720	-0.0118
	F	0.1073	0.5277	0.3709	-0.0060	0.1581	0.4637	0.3463	0.0317
	G	0.0398	0.4601	0.4601	0.0398	0.0872	0.4127	0.4127	0.0872
8	A	0.8049	0.3154	-0.0456	-0.0746	0.7493	0.3805	-0.0090	-0.1207
	B	0.6385	0.4021	0.0302	-0.0708	0.6144	0.4232	0.0602	-0.0978
	C	0.4794	0.4768	0.1078	-0.0641	0.4843	0.4586	0.1296	-0.0726
	D	0.3344	0.5277	0.1894	-0.0517	0.3630	0.4796	0.1999	-0.0426
	E	0.2134	0.5422	0.2752	-0.0309	0.2527	0.4788	0.2698	-0.0061
	F	0.1187	0.5128	0.3664	0.0019	0.1686	0.4512	0.3399	0.0401
	G	0.0501	0.4498	0.4498	0.0501	0.0973	0.4026	0.4026	0.0973

Table 12 (Continued)

Position of load (Grid No.) b	a	Effective slab width = 10' R_A	R_B	R_C	R_D	Effective slab width = 20' R_A	R_B	R_C	R_D
9	A	0.7955	0.3267	-0.0400	-0.0822	0.7408	0.3901	-0.0028	-0.1281
	B	0.6345	0.4054	0.0353	-0.0754	0.6106	0.4266	0.0646	-0.1020
	C	0.4805	0.4730	0.1122	-0.0658	0.4848	0.4565	0.1323	-0.0737
	D	0.3396	0.5186	0.1922	-0.0505	0.3671	0.4733	0.2004	-0.0408
	E	0.2211	0.5305	0.2753	-0.0271	0.2639	0.4700	0.2678	-0.0019
	F	0.1272	0.5019	0.3627	-0.0080	0.1761	0.4423	0.3352	0.0462
	G	0.0580	0.4419	0.4419	0.0580	0.1047	0.3952	0.0039	0.1047
10	A	0.7887	0.3348	-0.0359	-0.0876	0.7350	0.3966	0.0014	-0.1332
	B	0.6316	0.4079	0.0390	-0.0786	0.6080	0.4290	0.0677	-0.1048
	C	0.4812	0.4705	0.1151	-0.0669	0.4851	0.4552	0.1340	-0.0744
	D	0.3431	0.5124	0.1939	-0.0496	0.3699	0.4690	0.2006	-0.0396
	E	0.2265	0.5225	0.2752	-0.0243	0.2684	0.4641	0.2664	0.0010
	F	0.1333	0.4943	0.3598	0.0125	0.1813	0.4362	0.3318	0.0505
	G	0.0637	0.4362	0.4362	0.0637	0.1098	0.3901	0.0039	0.1098
11	A	0.7844	0.3399	-0.0332	-0.0911	0.7313	0.4008	0.0042	-0.1364
	B	0.6298	0.4095	0.0413	-0.0807	0.6063	0.4306	0.0697	-0.1066
	C	0.4816	0.4690	0.1169	-0.0676	0.4853	0.4544	0.1351	-0.0748
	D	0.3454	0.5085	0.1949	-0.0489	0.3716	0.4663	0.2007	-0.0387
	E	0.2300	0.5175	0.2749	-0.0224	0.2712	0.4604	0.2654	0.0028
	F	0.1372	0.4894	0.3578	0.0154	0.1846	0.4324	0.3296	0.0532
	G	0.0673	0.4326	0.4326	0.0673	0.1130	0.3869	0.0038	0.1130

Table 12 (Continued)

Position of load (Grid No.) b	a	Effective slab width = 10' R_A	R_B	R_C	R_D	Effective slab width = 20' R_A	R_B	R_C	R_D
12	A	0.7823	0.3423	-0.0318	-0.0929	0.7295	0.4028	0.0056	-0.1380
	B	0.6289	0.4103	0.0425	-0.0817	0.6055	0.4313	0.0706	-0.1075
	C	0.4818	0.4683	0.1177	-0.0679	0.4854	0.4540	0.1356	-0.0750
	D	0.3465	0.5067	0.1953	-0.0486	0.3724	0.4651	0.2008	-0.0383
	E	0.2316	0.5150	0.2747	-0.0215	0.2725	0.4586	0.2649	0.0038
	F	0.1391	0.4870	0.3569	0.0168	0.1862	0.4306	0.3286	0.0545
	G	0.0691	0.4308	0.4308	0.0691	0.1145	0.3854	0.0038	0.1145
12.5	A	0.7820	0.3427	-0.0316	-0.0931	0.7293	0.4040	0.0057	-0.1382
	B	0.6288	0.4104	0.0426	-0.0819	0.6054	0.4314	0.0707	-0.1076
	C	0.4818	0.4682	0.1178	-0.0680	0.4854	0.4539	0.1356	-0.0751
	D	0.3466	0.5064	0.1954	-0.0486	0.3725	0.4649	0.2008	-0.0383
	E	0.2319	0.5147	0.2747	0.0214	0.2727	0.4584	0.2649	0.0039
	F	0.1393	0.4868	0.3567	0.0170	0.1864	0.4303	0.3284	0.0547
	G	0.0693	0.4306	0.4306	0.0693	0.1147	0.3852	0.3852	0.1147

Table 13. Influence tables for reactions from slab to beams for single concentrated load. Ten foot bridge

(For midspan position)

Position of load (Grid No.) b	a	Effective slab width = 5' R_A	R_B	R_C	R_D	Effective slab width = 8' R_A	R_B	R_C	R_D
5	A	0.9212	0.1512	-0.0663	-0.0062	0.8942	0.1924	-0.0676	-0.0190
	B	0.6824	0.3650	-0.0274	-0.0200	0.6758	0.3656	-0.0088	-0.0326
	C	0.4584	0.5503	0.0239	-0.0327	0.4699	0.5161	0.0578	-0.0439
	D	0.2629	0.6794	0.1007	-0.0431	0.2877	0.6220	0.1409	-0.0508
	E	0.1139	0.7222	0.2137	-0.0499	0.1449	0.6592	0.2468	-0.0509
	F	0.0182	0.6634	0.3683	-0.0500	0.0469	0.6153	0.3785	-0.0408
	G	-0.0318	0.5318	0.5318	-0.0318	-0.0116	0.5116	0.5116	-0.0116